Part I

Materials

1

Extreme Mechanics of Hydrogels Toward *In Situ* Hydrogel Bioelectronics

Tsz H. Wong[1], Xuanhe Zhao[2,3], and Shaoting Lin[4]

[1]*Michigan State University, Department of Biomedical Engineering, 775 Woodlot Dr., East Lansing, MI 48824, USA*
[2]*Massachusetts Institute of Technology, Department of Mechanical Engineering, 77 Massachusetts Avenue, Cambridge, MA 02139, USA*
[3]*Massachusetts Institute of Technology, Department of Civil and Environmental Engineering, 77 Massachusetts Avenue, Cambridge, MA 02139, USA*
[4]*Michigan State University, Department of Mechanical Engineering, 474 S Shaw Ln, East Lansing, MI 48824, USA*

1.1 Introduction

In-situ bioelectronics, a rapidly evolving field focusing on the development of electronic devices that can operate within the body for on-site sensing, stimulation, and powering, holds great promise for revolutionizing the field of medicine in a variety of ways (Figure 1.1a) [1, 2]. For example, the development of biosensors that can achieve on-site quantification of biomarkers closely related to the development and progression of colorectal cancer (CRC) would enable early CRC detection preventing CRC from progressing, thereby increasing the five-year relative survival rate up to 90% [3]. The development of neural probes that can form intimate interfaces with neurons without provoking a severe foreign body response would enable chronic neuron stimulation and recording, facilitating fundamental understanding of neural activities and offering long-term treatment for neuropsychiatric disorders, traumatic injuries, and inflammatory conditions [4–6]. The advancement of energy harvesting devices that can provide sustainable power supply to cardiac pacemakers could prolong their lifespan and help maintain or restore a normal heart rhythm with electrical impulses [7–9]. However, the key challenge faced by *in-situ* bioelectronics stems from the fundamentally contradictory properties between electronic components and biological systems, which induce foreign body responses due to mechanical, chemical, and biological mismatches. Specifically, electronic components are typically made of metals, silicon, glass, ceramics, and plastics that are hard, dry, and abiotic; in contrast, biological systems are composed of living tissues that are soft, wet, and dynamic.

Hydrogels, as polymer networks infiltrated with water, exhibit intriguing multiphysics phenomena associated with mechanical, electrical, chemical, and thermal

Mechanics of Flexible and Stretchable Electronics, First Edition. Edited by Yong Zhu and Nanshu Lu.
© 2025 WILEY-VCH GmbH. Published 2025 by WILEY-VCH GmbH.

10.1002/9783527842308.ch1, Downloaded from https://onlinelibrary.wiley.com/doi/10.1002/9783527842308.ch1 by Michigan State University, Wiley Online Library on [05/09/2024]. See the Terms and Conditions (https://onlinelibrary.wiley.com/terms-and-conditions) on Wiley Online Library for rules of use; OA articles are governed by the applicable Creative Commons License

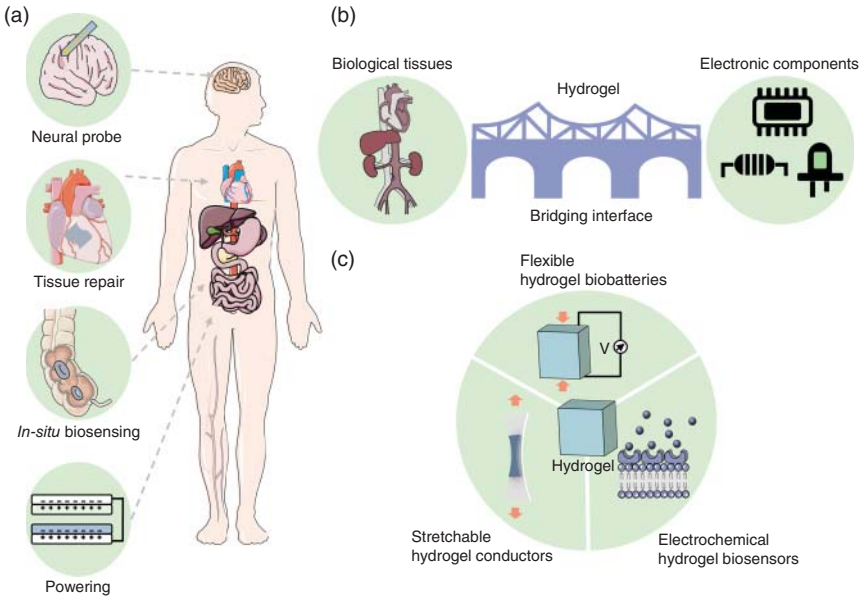


Figure 1.1 Overview of the *in-situ* hydrogel electronics. (a) *In-situ* bioelectronics revolutionized the field of medicine in a variety of ways. (b) Hydrogels form long-term, high-efficacy, multi-modal bridging interfaces between electronic components and biological systems. (c) Three key components of *in-situ* hydrogel bioelectronics include stretchable hydrogel conductors, electrochemical hydrogel biosensors, and flexible hydrogel biobatteries.

couplings [10, 11]. Hydrogels are typically constituted of two phases: one phase of interconnected polymer networks giving the solid-like network elasticity, and the other phase of infiltrated water molecules endowing the fluid-like transport property [12–15]. Due to the unique combination of polymer networks and water molecules, hydrogels show their superior softness, wetness, responsiveness, biocompatibility, and bioactivity, therefore having been regarded as an ideal material candidate to form long-term, high-efficacy, multi-modal bridging interfaces between electronic components and biological systems (Figure 1.1b) [16, 17].

Recently, a nascent field named hydrogel bioelectronics has rapidly evolved, exploiting hydrogels as key components for electronic devices that seamlessly interact with biological systems. The generic idea for the design of hydrogel bioelectronic device is to embed functional electronic components such as conductors, microchips, transducers, resistors, and capacitors inside or attached to the surface of a highly stretchable and tough hydrogel matrix, providing a soft, wet, and biocompatible environment interfacing with biological tissues [18]. As the hydrogel bioelectronic device is stretched, flexible electronic components can deform together with the device while rigid electronic components maintain their undeformed shapes, which involves large deformation of hydrogels around rigid electronic components [19, 20]. Therefore, to maintain reliability and functionality of the device, the hydrogel matrix and the interface between hydrogel and

10.1002/9783527842308.ch1, Downloaded from https://onlinelibrary.wiley.com/doi/10.1002/9783527842308.ch1 by Michigan State University, Wiley Online Library on [05/09/2024]. See the Terms and Conditions (https://onlinelibrary.wiley.com/terms-and-conditions) on Wiley Online Library for rules of use; OA articles are governed by the applicable Creative Commons License

functional components need to be tough and robust. Pioneered by Gong et al., hydrogels with fracture toughness higher than 10^4 J/m^2 have been widely available [21–23]; additionally, initiated in the past 10 years, hydrogel adhesions to diverse substrates can successfully achieve interfacial fracture toughness above 10^3 J/m^2, on the same order as their biological counterparts [24–29]. The recent development of tough hydrogels and tough hydrogel adhesions as well as their synthesis and fabrication techniques have enabled various soft material technologies in the form of diverse hydrogel bioelectronics [18, 30, 31].

More recently, an emerging class of *in-situ* bioelectronics that combines hydrogel technologies with electronic components to create devices that can interact with harsh environments within the body, which we define as *in-situ hydrogel bioelectronics*, have been recently proposed with great promise in potentially addressing the limitations faced by existing *in-situ* bioelectronics [16, 31, 32]. Despite the promise, the complicated chemical, biological, and mechanical factors in the physiological environment pose significant challenges to the reliability and functionality of hydrogel electronic devices when operating within the body. What are the key properties of hydrogels and how to rationally design these properties for developing electronic devices that can operate in the physiological environment for reliable on-site sensing, stimulation, and powering? These are unanswered questions, even considering a growing number of reviews on hydrogel bioelectronics [16, 33–37].

This chapter aims to provide an overview of the design principles, implementation mechanisms, and manufacturing/fabrication techniques, particularly centering on extreme mechanics of hydrogels, for developing three key components of *in-situ* hydrogel bioelectronics (Figure 1.1c): (i) stretchable hydrogel conductors, (ii) electrochemical hydrogel biosensors, and (iii) flexible hydrogel biobatteries. The chapter is organized as follows. Section 1.2 will discuss polymer mechanics for rationally designing extreme mechanical and physical properties of hydrogels crucial for the development of *in-situ* hydrogel bioelectronics. Section 1.3 will discuss the multiscale orthogonal design of stretchable hydrogel conductors and strategies for implementing the orthogonal design. Section 1.4 will discuss the principles for achieving high-specificity and high-sensitivity of electrochemical hydrogel biosensors, specifically focusing on selective transport design in hydrogels and electrochemical sensing performance at hydrogel–electrode interfaces. Section 1.5 will briefly review the recent efforts in developing flexible hydrogel biobatteries by harvesting mechanical energy, chemical energy, and thermal energy. Section 1.6 will conclude the chapter with a set of future opportunities by integrating interdisciplinary efforts in ingestible sensors, neural interfaces, miniature robots, and data analytics.

1.2 Extreme Properties of Hydrogels by Polymer Network Design

Due to the unique combination of solid-like polymer networks and fluid-like water molecules, hydrogels exhibit superior softness, wetness, responsiveness,

10.1002/9783527842308.ch1, Downloaded from https://onlinelibrary.wiley.com/doi/10.1002/9783527842308.ch1 by Michigan State University, Wiley Online Library on [05/09/2024]. See the Terms and Conditions (https://onlinelibrary.wiley.com/terms-and-conditions) on Wiley Online Library for rules of use; OA articles are governed by the applicable Creative Commons License

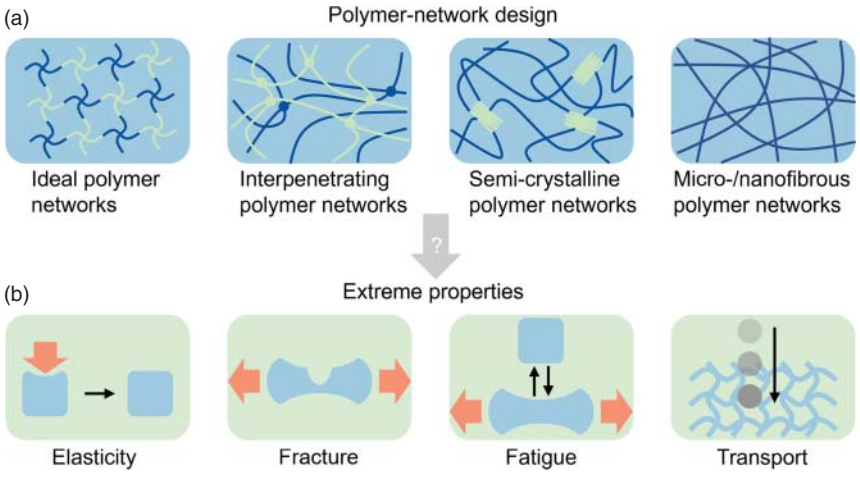


Figure 1.2 Extreme properties of hydrogels by polymer network design. (a) Schematics of unconventional polymer networks such as ideal polymer networks, interpenetrating polymer networks, semi-crystalline polymer networks, micro-/nanofibrous polymer networks. (b) Schematics of mechanical and physical properties critical for the development of *in-situ* hydrogel bioelectronics, including elasticity, fracture, fatigue, and mass transport.

biocompatibility, and bioactivity, therefore being exploited as key material candidates for developing *in-situ* hydrogel bioelectronics. These properties have been intensively studied by understanding the nonlinear elasticity [38], swelling [39–43], poroelasticity [44, 45], viscoelasticity [46–50], fracture [51–53], and fatigue [54–57] of hydrogels, following the pioneering work in the field of polymers and soft materials [58–69]. Despite these unique mechanical and physical properties of common hydrogels, the development of *in-situ* hydrogel bioelectronics also requires hydrogels to possess extreme mechanical and physical properties, such as tunable elastic modulus, extremely high values of fracture toughness and fatigue threshold, and tunable molecular transport. In this section, we will discuss the polymer mechanics to rationally push the limits of mechanical and physical properties of hydrogels including elastic modulus, fracture toughness, fatigue threshold, and mass transport that are crucial for the development of *in-situ* hydrogel bioelectronics (Figure 1.2).

1.2.1 Elastic Modulus

Elastic modulus is one of the most important properties of hydrogels used in biomedical applications, as it governs their ability to withstand deformations while maintaining compliance without damaging the surrounding soft tissues or causing adverse foreign body responses. There are several methods available to measure the elastic modulus of hydrogels, including tensile/compression, rheology, and indentation tests, as illustrated in Figure 1.3a. The shear elastic modulus of a hydrogel G can be measured by identifying the initial slope of the stress–strain curve in tensile or compression tests E, namely $G = \alpha E$, where α is a dimensionless perfector

10.1002/9783527842308.ch1, Downloaded from https://onlinelibrary.wiley.com/doi/10.1002/9783527842308.ch1 by Michigan State University, Wiley Online Library on [05/09/2024]. See the Terms and Conditions (https://onlinelibrary.wiley.com/terms-and-conditions) on Wiley Online Library for rules of use; OA articles are governed by the applicable Creative Commons License

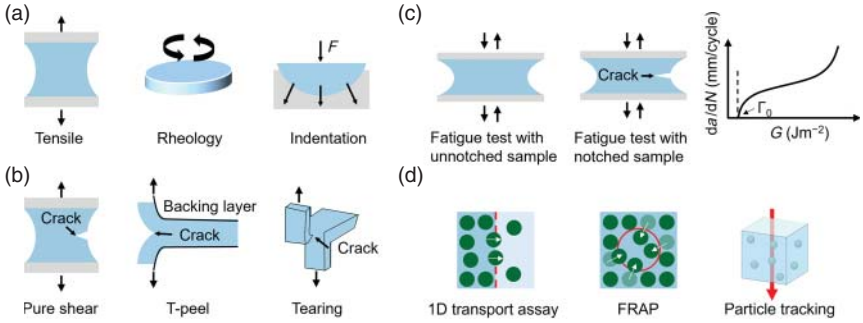


Figure 1.3 Common experimental methods to characterize mechanical and physical properties of hydrogels. (a) Tensile, rheology, and indentation tests to measure the elastic modulus of hydrogels. (b) Pure shear, T-peel, and tearing tests to measure the fracture toughness of hydrogels. (c) Pure shear fatigue tests to measure the fatigue threshold of hydrogels Γ_0 by plotting the crack extension da/dN versus the applied energy release rate G. (d) 1D transport assay, fluorescence recovery after photobleaching (FRAP), and particle tracking methods to measure the diffusivity of particles (e.g. ions, monomers, proteins, viruses) in hydrogels.

depending on samples' dimensions and material incompressibility [70]. Rheology test is the other method to measure the shear elastic modulus of a hydrogel, which is often preferred for soft hydrogels. Rheology tests can provide information on both storage and loss modulus across a range of frequencies, allowing for a quantitative decomposition of elastic and viscous contributions during deformation [71]. Indentation tests can also be used to characterize the shear elastic modulus, but the results may be affected by water migration and stress state. Therefore, a theoretical analysis is necessary to accurately interpret the indentation results and decouple nonlinear elasticity, viscoelasticity, and poroelasticity in hydrogels [72].

Assuming the polymer network of a hydrogel is fully amorphous with negligible molecular entanglements and crystalline domains, the shear elastic modulus of a hydrogel G can be theoretically predicted following the classical affine and phantom network theories of elasticity [12, 66],

$$\frac{G}{kT} = C\phi^{1/3}n \tag{1.1}$$

where ϕ is the volume fraction of dry polymers, n is the number of elastically active polymer chains per unit volume of dry polymers, k is the Boltzmann constant, T is the absolute temperature, and C is a constant that has a value of 1 when the polymer network of the hydrogel follows affine deformation and $1 - \frac{2}{f}$ when the polymer network of the hydrogel follows phantom deformation with f being the functionality of the polymer network (i.e. the number of chains connected to a junction point). By substituting the typical values of $C = 1$, $\phi = 0.1$, $n = 10^{24} - 10^{26}$ m^{-3}, and $kT = 4.11 \times 10^{-21}$ J, the shear elastic modulus of a hydrogel is estimated on the order of 1–100 kPa.

Recent experiments have shown that the measured shear modulus of a hydrogel is consistently below the theoretical predictions by Eq. (1.1) due to the presence of molecular defects in a real hydrogel. Given the capability of counting the numbers

10.1002/9783527842308.ch1, Downloaded from https://onlinelibrary.wiley.com/doi/10.1002/9783527842308.ch1 by Michigan State University, Wiley Online Library on [05/09/2024]. See the Terms and Conditions (https://onlinelibrary.wiley.com/terms-and-conditions) on Wiley Online Library for rules of use; OA articles are governed by the applicable Creative Commons License

of various orders of molecular defects in hydrogels, Olsen and Johnson and coworkers [73] developed a real elastic network theory to quantify the impact of molecular defects on shear elastic modulus,

$$\frac{G}{kT} = \frac{f-2}{f}\sum_i \varepsilon_i n_i \tag{1.2}$$

where n_i is the number of the type i polymer chains per unit volume of the hydrogel associated with a specific type of molecular defects, ε_i is the elastic effectiveness of the type i polymer chains. ε_i accounts for the elastic contribution of each polymer chain, having a value of 1 if the polymer chain is an ideal chain with no impact from defects and a value smaller than 1 if the polymer chain is a defective chain affected by surrounding molecular defects. The real elastic network theory suggests the critical role of polymer network architecture on hydrogel's elastic modulus. The design principle for achieving tunable elastic modulus of hydrogels is to engineer the type and density of molecular defects, ubiquitous in synthetic hydrogels and biological tissues [74] (Figure 1.4a).

1.2.2 Fracture Toughness

Fracture toughness, the energy required to propagate a unit area of crack surface under monotonic load, defines the ability of a material to resist crack extension under stress. Fracture toughness of a hydrogel is crucial for maintaining reliability of *in-situ* hydrogel bioelectronics [10, 11]. As illustrated in Figure 1.3b, the fracture toughness of a hydrogel can be measured through pure shear, T-peel, and tearing tests, originally proposed by Rivlin and Thomas for measuring the fracture toughness of rubbers [75]. In a pure shear test, the fracture toughness of a hydrogel Γ is determined by the critical energy release rate applied on a notched sample G_c, $\Gamma = G_c = W(\lambda_c)H$, where W is the strain energy density stored in the unnotched sample with λ_c being the critical stretch for crack extension in the notched sample, and H is the sample height [53]. T-peel tests can also be used to measure the fracture toughness of hydrogels [76], where a hydrogel layer with a precut is sandwiched between two inextensible backing layers. The fracture toughness of the hydrogel is then calculated via $\Gamma = 2F_{SS}/b$, where F_{SS} is the steady-state plateau force, and b is the specimen's thickness. Tearing tests, also known as trouser tests, are another commonly adopted method for measuring hydrogel toughness [77]. Unlike pure shear and T-peel tests with the crack deformed in Mode I, the crack in a tearing test is deformed in Mode III (out-of-plane shear loading). The fracture toughness of a hydrogel in a tearing test is determined by $\Gamma = 2F_{SS}/b$, where F_{SS} is the steady-state plateau force, and b is the specimen's thickness.

Common hydrogels are intrinsically brittle [78]. The intrinsic fracture energy of a hydrogel Γ_0 can be calculated following the classical Lake–Thomas theory [12, 61, 79],

$$\Gamma_0 = \phi^{2/3} \cdot n\sqrt{N}b \cdot NU = \phi^{2/3} nbN^{3/2}U \tag{1.3}$$

where ϕ is the volume fraction of dry polymers, $n\sqrt{N}b$ is the number of elastically active polymer chains per unit area of crack surface, with n being the number of

10.1002/9783527842308.ch1, Downloaded from https://onlinelibrary.wiley.com/doi/10.1002/9783527842308.ch1 by Michigan State University, Wiley Online Library on [05/09/2024]. See the Terms and Conditions (https://onlinelibrary.wiley.com/terms-and-conditions) on Wiley Online Library for rules of use; OA articles are governed by the applicable Creative Commons License

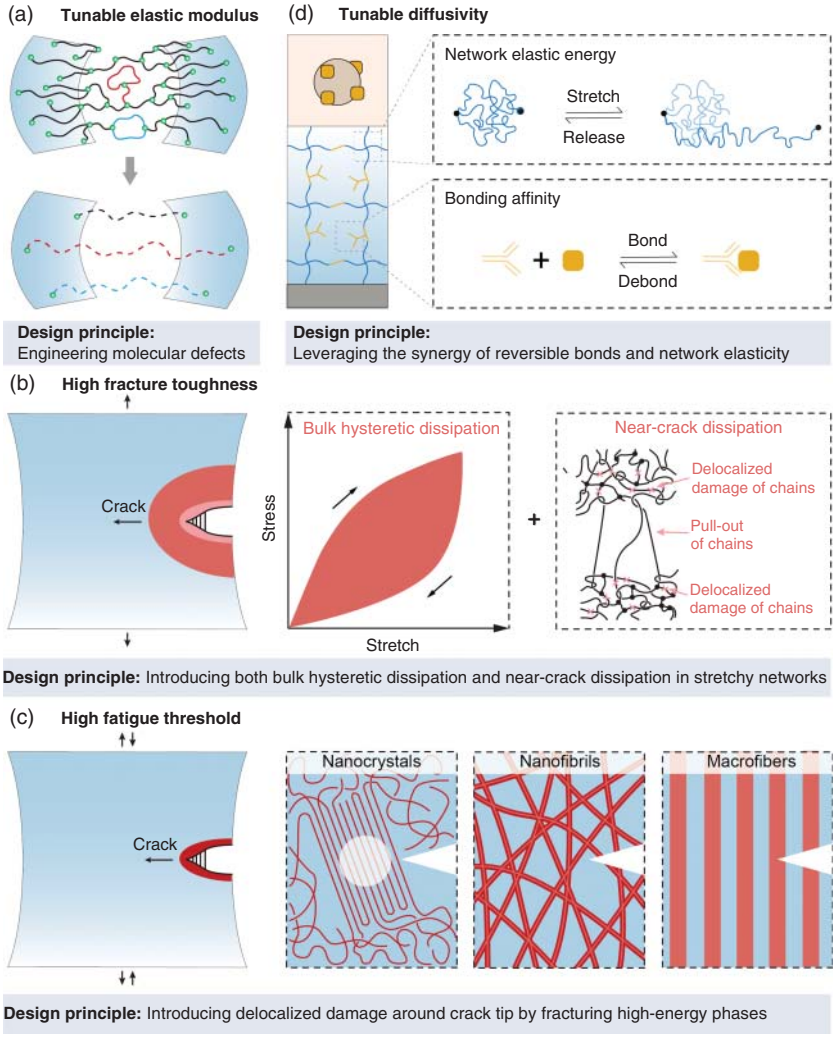


Figure 1.4 Design principles for extreme properties of hydrogels. (a) Achieving tunable elastic modulus by engineering type and density of molecular defects in hydrogels. (b) Achieving high fracture toughness of hydrogels by introducing both bulk hysteretic dissipation and near-crack dissipation in stretchy polymer networks. (c) Achieving high fatigue threshold of hydrogels by introducing high-energy phases to impinge fatigue crack extension. (d) Achieving tunable diffusivity in hydrogels by leveraging the synergy of reversible bonds and network elasticity.

elastically active polymer chains per unit volume of dry polymers, N being the number of Kuhn monomers in each polymer chain, b being the length of each Kuhn monomer, NU is the energy required to fracture a polymer chain, with U being the energy required to fracture a single Kuhn monomer. It is commonly assumed that the dry polymers of a hydrogel satisfy the volume conservation following $Nnb^3 = 1$ with b^3 being the volume of a Kuhn monomer. By imposing the volume conservation, the

10.1002/9783527842308.ch1, Downloaded from https://onlinelibrary.wiley.com/doi/10.1002/9783527842308.ch1 by Michigan State University, Wiley Online Library on [05/09/2024]. See the Terms and Conditions (https://onlinelibrary.wiley.com/terms-and-conditions) on Wiley Online Library for rules of use; OA articles are governed by the applicable Creative Commons License

intrinsic fracture energy of a hydrogel can be calculated via,

$$\Gamma_0 = \phi^{2/3} b^{-2} N^{1/2} U \tag{1.4}$$

By substituting the typical values of $\phi = 0.1$, $b = 10^{-9}$ m, $N = 100 - 10,000$, and $U = 100\text{kT} = 4.11 \times 10^{-19}$ J, the intrinsic fracture energy of a hydrogel Γ_0 is estimated as low as 1–10 J/m^2, orders of magnitude lower than biological tissues around 1000 J/m^2.

Lin and Zhao recently developed a defect-network fracture model to predict the intrinsic fracture energy of polymer networks containing various types of topological defects including cyclic loops and dangling chains [80]. The defect-network fracture model is inspired by the real elastic network model [73] or, more generally, the phantom network model [66, 81] discussed in Section 1.2.1. Analogous to the previous elastic models, the key idea of this fracture model is to introduce effectively longer fractured chains to account for the energy of the fractured chains on the crack path. However, physically different from the previous elastic models, the effectively longer chains in the fracture model do not change the density of the layer of fractured chains. The intrinsic fracture energy of the polymer network with defects normalized by that of the corresponding defect-free ideal network can be expressed as:

$$\overline{\Gamma} = \sum_X (\gamma_X - 1) n_X^{\text{affected}} - \sum_X n_X^{\text{inactive}} + 1 \tag{1.5}$$

where $\gamma_X \geq 1$ is the fracture effectiveness to account for the contribution to intrinsic fracture toughness by a single polymer chain affected by defect X, n_X^{affected} is the number density of affected chains due to the presence of defect X, n_X^{inactive} is the number density of inactive chains due to the presence of defect X. The defect-network fracture model indicates a competing effect due to the presence of topological defects: toughening by increasing effective chain length and weakening by introducing inactive chains. While the defect-network fracture model predicts that the presence of defects can potentially enhance intrinsic fracture energy of hydrogels by a few times, such enhancement is not sufficient to ensure the reliable use of hydrogels in engineering applications.

In the past 20 years, the fracture toughness of hydrogels has been significantly enhanced above 1000 J/m^2, making tough hydrogels key load-bearing components for devices and machines [82, 83]. The generic toughening mechanism of hydrogels is to incorporate two physical processes: one is the scission of a layer of polymer chains on the crack tip, and the other is the bulk hysteretic dissipation around the crack tip such as Mullins effect and viscoelasticity [22, 23, 51, 78, 84–91]. The first process defines the intrinsic fracture energy Γ_0 as discussed in Eqs. (1.3)–(1.5), and the second process defines the bulk hysteretic dissipation's contribution Γ_D^{bulk}. Conceptually, the total fracture toughness of a tough hydrogel can be expressed as:

$$\Gamma = \Gamma_0 + \Gamma_D^{\text{bulk}} \tag{1.6}$$

which is often named the bulk dissipation model. The value of Γ_D^{bulk} can be estimated by $\Gamma_D^{\text{bulk}} = U_D L_D$ with U_D being the energy for breaking sacrificial bonds per unit volume of the material and L_D being the length of the process zone around crack tip where breaking sacrificial bonds occurs. U_D can be estimated by the bond

10.1002/9783527842308.ch1, Downloaded from https://onlinelibrary.wiley.com/doi/10.1002/9783527842308.ch1 by Michigan State University, Wiley Online Library on [05/09/2024]. See the Terms and Conditions (https://onlinelibrary.wiley.com/terms-and-conditions) on Wiley Online Library for rules of use; OA articles are governed by the applicable Creative Commons License

energy of one sacrificial bond times the number of sacrificial bonds per unit volume of the material, on the order of $10^6\,J/m^3$. Since the value of L_D can reach 1 mm [92], the value of Γ_D^{bulk} can reach $1000\,J/m^2$, with the orders of magnitude larger than Γ_0.

The bulk dissipation model has been widely used to qualitatively explain the toughening mechanisms in diverse soft tough materials [21, 23, 93–95], but recent study shows that the bulk dissipation model significantly underestimates the toughness enhancement of tough hydrogels [93]. The missing term is attributed to a near-crack dissipation that does not rely on bulk hysteresis [96–98]. To account for both bulk hysteretic dissipation and near-crack dissipation in soft tough materials, an extreme toughening model was recently proposed, indicating that the total fracture toughness of a tough hydrogel exhibiting both bulk hysteretic dissipation and near-crack dissipation can be expressed as:

$$\Gamma = \Gamma_0 + \Gamma_D^{bulk} + \Gamma_D^{tip} \tag{1.7}$$

where Γ_0 is the intrinsic fracture energy, Γ_D^{bulk} is the bulk hysteretic dissipation's contribution to fracture toughness, and Γ_D^{tip} is the near-crack dissipation's contribution to fracture toughness. A governing equation for the extreme toughening model can be further derived as:

$$\frac{\Gamma}{\Gamma_0} = \frac{\beta}{1 - \alpha h_m} \tag{1.8}$$

where $\beta = \left(\Gamma_0 + \Gamma_D^{tip}\right)/\Gamma_0 \geq 1$ is a dimensionless number to account for the near-crack dissipation due to molecular entanglements, $0 \leq \alpha \leq 1$ is a dimensionless number depending on the stretch-dependent hysteresis of the bulk materials ($\alpha = 1$ for highly stretchable materials), and $0 \leq h_m < 1$ is the maximum stress-stretch hysteresis of the bulk material. While the cause of the near-crack dissipation is not fully understood, the reported experiments have shown the potential for achieving high values of β up to 10, suggesting the crucial toughening role by the near-crack dissipation. To summarize, the design principle for achieving high fracture toughness in hydrogels is to introduce both bulk hysteretic dissipation (e.g. Mullins effect and viscoelasticity) and near-crack dissipation (e.g. molecular entanglements) in stretchy polymer networks, as depicted in Figure 1.4b.

1.2.3 Fatigue Threshold

Fatigue threshold, the energy required to propagate a unit area of crack surface under cyclic load, defines the ability of a material to resist fatigue crack extension under stress [55, 99, 100]. Fatigue threshold of hydrogels is critical for achieving longevity of *in-situ* hydrogel bioelectronics. As illustrated in Figure 1.3c, the measurement of fatigue threshold of hydrogels requires cyclic loading of unnotched and notched hydrogel specimens. The fatigue tests for hydrogels are typically performed in a chamber with controlled humidity or water bath to ensure the sample reaches an equilibrium state [54, 56]. By monitoring the crack extension Δa at a controlled

10.1002/9783527842308.ch1, Downloaded from https://onlinelibrary.wiley.com/doi/10.1002/9783527842308.ch1 by Michigan State University, Wiley Online Library on [05/09/2024]. See the Terms and Conditions (https://onlinelibrary.wiley.com/terms-and-conditions) on Wiley Online Library for rules of use; OA articles are governed by the applicable Creative Commons License

energy release rate G, one can identify a critical energy release rate at the intersection of abscissa axis as the measured fatigue threshold Γ_0.

While hydrogels have been made tough with high toughness above 1000 J/m^2, as discussed in Section 1.2.2, these tough hydrogels still suffer from fatigue fracture when subjected to prolonged cyclic loading [54, 79, 97, 101]. The experimental findings conclude that the resistance to fatigue crack propagation after prolonged cycles of loads is the energy required to fracture a single layer of polymer chains (i.e. the intrinsic fracture energy of the hydrogel), which is unaffected by the additional dissipation mechanisms introduced in tough hydrogels [56]. To address the challenge of fatigue failures in conventional tough hydrogels, we and others have proposed a general design principle for fatigue-resistant hydrogels (Figure 1.4c) – inducing delocalized damage around the crack tip by fracturing high-energy phases, such as nanocrystals [28, 56, 100, 102–104], micro−/nanofibers [105], and macro-fibers [92, 106] in hydrogels. Additionally, hierarchical molecular structure design such as introducing bi-continuous phase networks can suppress fatigue-induced crack advance [57, 107].

The fatigue threshold of fatigue-resistant hydrogels containing high-energy phases can be qualitatively calculated by modifying the Lake–Thomas theory:

$$\Gamma_0 = \phi^{2/3} n l_d N U \tag{1.9}$$

where ϕ is the volume fraction of dry polymers, n is the number of elastically active polymer chains per unit volume of dry polymers, NU is the energy required to fracture a polymer chain with N being the number of Kuhn monomers in each polymer, U being the energy required to fracture a single Kuhn monomer, and l_d is the length scale of the delocalized damage and understood as the crack processing zone length at the threshold. In conventional hydrogels, l_d is equal to the length of a single layer of polymer chains, i.e. $l_d = \sqrt{Nb}$; in fatigue-resistant hydrogels, l_d is larger than the length of a single layer of polymer chains, i.e. $l_d > \sqrt{Nb}$. Since the parameters ϕ, N, and U are intrinsic properties of hydrogels with little room to engineer, the strategies to enhance fatigue threshold of hydrogels mainly rely on the mechanisms that can significantly enlarge the value of l_d, which can be achieved by introducing intrinsically high-energy phases above mentioned.

1.2.4 Mass Transport

Diffusion in a hydrogel, movement of particles (e.g. ions, monomers, proteins, and viruses) through the hydrogel, is a ubiquitous phenomenon in nature and a fundamental process that governs the working principles in diverse applications. For example, the distinct diffusion of different biomarkers in hydrogels determines the sensing sensitivity and sensing specificity in electrochemical hydrogel biosensors discussed in Section 1.4; the stress-induced diffusion of ions in nano channels of hydrogels governs the stress-voltage coupling in flexible hydrogel batteries discussed in Section 1.5. The diffusivity of particles in hydrogels can be commonly characterized by 1D transport assay, fluorescence recovery after bleaching (FRAP), and particle tracking methods (Figure 1.3d).

10.1002/9783527842308.ch1, Downloaded from https://onlinelibrary.wiley.com/doi/10.1002/9783527842308.ch1 by Michigan State University, Wiley Online Library on [05/09/2024]. See the Terms and Conditions (https://onlinelibrary.wiley.com/terms-and-conditions) on Wiley Online Library for rules of use; OA articles are governed by the applicable Creative Commons License

The mode of diffusion in a hydrogel is determined by the mesh size of the hydrogel. When the hydrogel's mesh size is much larger than the size of the substance, the substance moves as Brownian diffusion, the diffusivity of which is governed by the viscosity of solvent (i.e. water) in the hydrogel [108]:

$$D = \frac{kT}{3\pi\eta d} \tag{1.10}$$

where k is the Boltzmann constant, T is the absolute temperature, η is the dynamic viscosity of water, and d is the diameter of the substance. By substituting the typical values of $kT = 4.21 \times 10^{-21}$ J, $\eta = 8.9 \times 10^{-4}$ Pa · s, and $d = 1$ nm, the diffusivity of the substance in a hydrogel with large mesh size is estimated as 10^{-10} m/s^2. When the hydrogel's mesh size is on the same order as the size of the substance, the diffusivity of the substance in a hydrogel is governed by the hydrogel's mesh size ξ [109]:

$$\frac{D}{D_0} \sim \exp\left(-\frac{d}{\xi}\right) \tag{1.11}$$

where D_0 is the diffusivity of the substance in water. For a hydrogel with its mesh size two times the substance diameter (i.e. $d/\xi = 2$), the diffusivity of the substance reduces by 10 times on the order of 10^{-11} m/s^2 .

Existing efforts have been mostly focused on Brownian diffusion of particles in a fluid, the diffusivity of which is governed by the viscosity of fluids. In contrast, when particles diffuse in the polymer networks of a hydrogel, the transport of particles is a discrete process of particles making stochastic hops between neighboring sites, namely hopping diffusion, the diffusivity of which is governed by the energy required to overcome the elasticity of polymer networks [110]. Such network elasticity can be readily tuned by mechanical deformation applied on the hydrogel. This implies the potential of harnessing mechanical deformation as a new design space to program particle transport in hydrogels. Specifically, for a particle with size d confined in a cage formed by polymer chains with mesh size ξ slightly smaller than particle size (i.e. $\xi < d$), the particle can still escape from one cage to the other neighboring cage by overcoming the energy barrier due to network elasticity. The probability for such escape P is determined by the energy barrier E_e via $P = \int_d^\infty \frac{e^{-E_e/kT}}{\xi}\,\mathrm{d}x$ where k is the Boltzmann constant and T is the absolute temperature, resulting in a reduced hopping diffusivity [110],

$$D_{\text{network}} = D_0 P \tag{1.12}$$

where D_0 is the particle diffusivity in a hydrogel free of network elasticity. The fundamental understanding of how mechanical deformation modulates particle transport in soft materials remains an unexplored research topic but will potentially lead to multiple previously inaccessible technologies that rely on mechano-transport design in hydrogels, including but not limited to force-sensitive cargo for on-demand drug delivery, and strain-programmable tissue adhesive for prolonged tissue repair.

In addition to network elasticity, hopping diffusion in hydrogels can also be induced by reversible interactions between particles and functional groups in hydrogels [111]. During a hopping event, multipoint particle attachment results in caging. As one or more of the attached points can be released, the particle can escape from one cage to the other neighboring cage, resulting in hopping

10.1002/9783527842308.ch1, Downloaded from https://onlinelibrary.wiley.com/doi/10.1002/9783527842308.ch1 by Michigan State University, Wiley Online Library on [05/09/2024]. See the Terms and Conditions (https://onlinelibrary.wiley.com/terms-and-conditions) on Wiley Online Library for rules of use; OA articles are governed by the applicable Creative Commons License

diffusivity,

$$D_{\text{reversible}} = \sum_{j=2}^{N} k_{\text{off}} P_j D_0. \tag{1.13}$$

where P_j is the probability of a particle maintaining j number of bonding sites, N is the number of bonding sites on the particle, D_0 is the particle diffusivity with one bonding site ($N = 1$), and k_{off} is the dissociate rate of the reversible interaction. Harnessing hopping diffusion by reversible interactions enables selective transport of chemical and biological cargoes based on reversible cargo-barrier interactions [112, 113]. Overall, the principle to tune particle diffusivity in hydrogels is to leverage the synergy of network elasticity and reversible bonds (Figure 1.4d).

1.3 Stretchable Hydrogel Conductors

Hydrogel-based electronic materials that can conduct electricity while being able to stretch and deform without fracture, known as stretchable hydrogel conductors, hold great potential as an alternative to traditional metallic conductors in the development of *in-situ* hydrogel bioelectronics due to their unique combination of tissue-like properties and electrical conductivity [18, 114]. Despite the promising potential, existing stretchable hydrogel conductors face a technical challenge in reconciling superior mechanical toughness and high electrical conductivity, limiting their use in *in-situ* hydrogel bioelectronics that require both mechanical and electrical properties [115–117]. Currently, most stretchable hydrogel conductors consist of a mixture of electrically conductive fillers in stretchable hydrogel matrices, resulting in low electrical conductivity due to low connectivity between electrical phases in the hydrogel matrices. Although increasing the amount of conductive filler can improve the electrical conductivity by forming a percolation network, this approach significantly compromises the hydrogel's mechanical properties by reducing stretchability and fracture toughness.

1.3.1 Multiscale Orthogonal Design

The design principle of stretchable hydrogel conductors is depicted in Figure 1.5, where the integration of electrical and mechanical phases is accomplished by a bi-continuous structure with an orthogonal design of each phase. To achieve high electrical conductivity, various electrical fillers such as ions [118, 119], conductive monomers [120, 121], conductive polymers [122–124], conductive nanoparticles [125, 126], and conductive macro fillers [127, 128] have been used. On the other hand, to achieve superior mechanical elasticity, stretchable hydrogels with interpenetrating polymer networks [21, 23, 129], hybrid crosslinkers [130–132], high-functionality crosslinkers [133–135], monodispersed polymer chains [136, 137], and meso-/macro composites [138–140] have been designed. While high electrical conductivity and superior mechanical elasticity have been

10.1002/9783527842308.ch1, Downloaded from https://onlinelibrary.wiley.com/doi/10.1002/9783527842308.ch1 by Michigan State University, Wiley Online Library on [05/09/2024]. See the Terms and Conditions (https://onlinelibrary.wiley.com/terms-and-conditions) on Wiley Online Library for rules of use; OA articles are governed by the applicable Creative Commons License

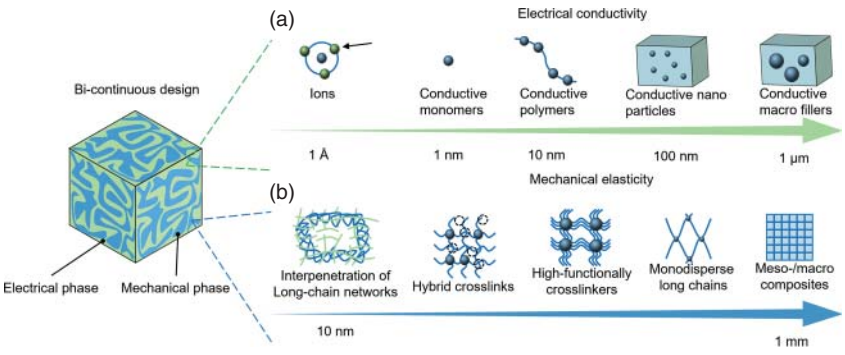


Figure 1.5 Design of stretchable hydrogel conductors relying on a bi-continuous integration of electrical and mechanical phases. (a) The high electrical conductivity in the electrical phase can be achieved by introducing electrical fillers including ions, conductive monomers, conductive polymers, conductive nanoparticles, and conductive macro fillers. (b) The superior mechanical elasticity in the mechanical phase can be achieved by designing stretchable hydrogels with interpenetrating polymer networks, hybrid crosslinkers, high-functionality crosslinkers, monodispersed polymer chains, and meso-/macro composites. Source: Reproduced with permission from Ref. [78]. Copyright 2014 The Royal Society of Chemistry.

demonstrated individually, the integration of these two phases is challenging due to their significant mechanical mismatch. The elastic modulus of the electrical phase (~1 GPa) is typically much larger than that of the mechanical phase (hydrogels, ~1–100 kPa), leading to stress concentrations at their interface and surface delamination when highly deformed. Furthermore, the fracture toughness of the electrical phase (~10 J/m^2) is typically much lower than that of the mechanical phase (tough hydrogels, 1000 J/m^2), resulting in microcrack formation and decreased electrical conductivity. Despite numerous individual efforts to enhance electrical conductivity and mechanical elasticity, implementing the orthogonal design through the bi-continuous integration of the electrical and mechanical phases remains a challenge.

1.3.2 Implementations of the Orthogonal Design

Figure 1.6 illustrates the typical ways in which the orthogonal design of stretchable hydrogel conductors can be implemented. A biocompatible, highly stretchable, and robust hydrogel provides a soft and wet matrix for electronic components, drastically different from dry elastomer/polymer matrices used in conventional stretchable electronics. Electronic components including stretchable, rigid, and brittle conductors are either embedded inside or attached to the surface of the hydrogel. When the stretchable hydrogel conductor is stretched, stretchable electronic components can deform together with the conductor, while rigid electronic components maintain their undeformed shapes, which requires robust interfaces between electronic components and hydrogel

10.1002/9783527842308.ch1, Downloaded from https://onlinelibrary.wiley.com/doi/10.1002/9783527842308.ch1 by Michigan State University, Wiley Online Library on [05/09/2024]. See the Terms and Conditions (https://onlinelibrary.wiley.com/terms-and-conditions) on Wiley Online Library for rules of use; OA articles are governed by the applicable Creative Commons License

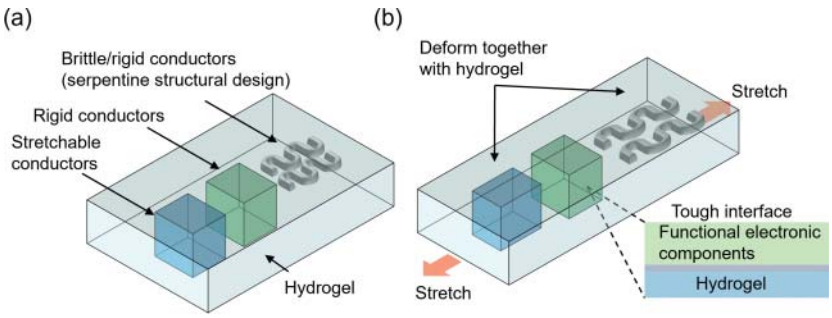


Figure 1.6 General strategies to implement the orthogonal design of stretchable hydrogel conductors. (a) Electronic components including stretchable, rigid, and brittle conductors are embedded inside or attached on the surface of the hydrogel. (b) As the stretchable hydrogel conductor is stretched, stretchable electronic components can deform together with the conductor, but rigid electronic components maintain their undeformed shapes, which requires robust interfaces between electronic components and hydrogel matrix. Additionally, brittle electronic components require serpentine structural designs to reduce the energy for driving the crack formation in electronic components. Source: Reproduced with permission from Ref. [18]. Copyright 2015 John Wiley & Sons, Inc.

matrix. In addition, brittle electronic components require serpentine structural designs to minimize the energy for driving crack formation in the electronic components.

While a stretchable hydrogel conductor with intrinsically stretchable electronic components does not require special interfacial or structural design, it requires material innovation for the design of intrinsically stretchable conductive materials. Conventional conductive materials have difficulty forming long-term stable and conformable interfaces with both biological and synthetic hydrogels due to severe modulus mismatch. For example, carbon-based conductive materials like graphene have moduli of 1 TPa; metallic conductive materials like silicon have moduli of 50 GPa; even conducting polymers such as poly(3,4-ethylenedioxythiophene) polystyrene sulfonate (PEDOT: PSS), polyaniline (PANI), and polypyrrole (PPy), possessing superior flexibility compared to inorganic conductors, typically have moduli on the order of 1 GPa [141]. PEDOT: PSS-based hydrogels [13, 142], owing to their favorable compatibility, processability, and reproducibility, represent one of the most common material candidates for intrinsically stretchable electronic components. Figure 1.7a summarizes the recent efforts in reconciling electrical conductivity and mechanical stretchability in PEDOT: PSS hydrogels through interpenetrating polymer networks [142], dispersing conductive nanofillers [148], and engineering PEDOT: PSS nanofibrils [13, 149]. Liquid metal, a metal alloy including gallium, indium, and tin, is another class of intrinsically stretchable conductive materials, recently embedded in hydrogels [150, 151]. Although liquid metal shows unique properties such as high conductivity, excellent thermal stability, and ease of processing, it is also corrosive, reactive with water or oxygen, and requires safety precautions.

10.1002/9783527842308.ch1, Downloaded from https://onlinelibrary.wiley.com/doi/10.1002/9783527842308.ch1 by Michigan State University, Wiley Online Library on [05/09/2024]. See the Terms and Conditions (https://onlinelibrary.wiley.com/terms-and-conditions) on Wiley Online Library for rules of use; OA articles are governed by the applicable Creative Commons License

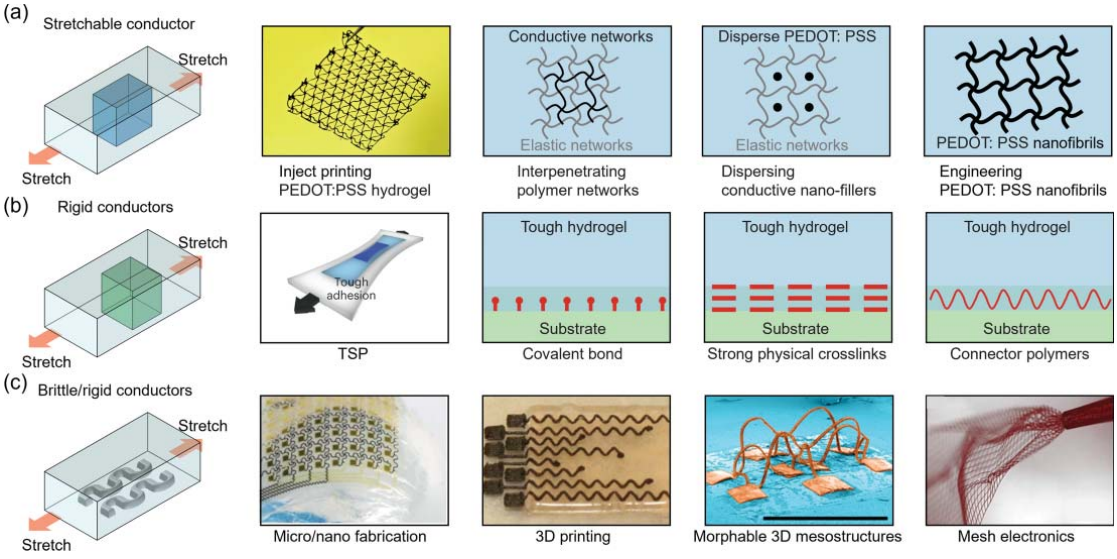


Figure 1.7 Representative examples to implement the orthogonal design of stretchable hydrogel conductors. (a) The implementation of a stretchable hydrogel conductor with stretchable conductors requires material innovations for the design of intrinsically stretchable conductive materials such as PEDOT: PSS-based hydrogels shown in the left image (Source: Ref. [13]/Springer Nature/CC BY 4.0). The design of PEDOT: PSS hydrogels typically relies on interpenetrating polymer networks, dispersing conductive nanofillers, and engineering PEDOT: PSS nanofibrils. (b) The implementation of a stretchable hydrogel conductor with rigid conductors requires strong and tough interfaces between the electronic components and the hydrogel matrix such as TSP recently developed by Jin and Bao and coworkers shown in the left image (Source: Reproduced with permission from Ref. [143]. Copyright 2022 Springer Nature). The design of strong and tough interfaces typically relies on covalent bonds, strong physical crosslinks, and connector polymers. (c) The implementation of a stretchable hydrogel conductor with brittle/rigid conductors also requires serpentine structural design, which typically relies on advanced manufacturing techniques such as micro-/nanofabrication (Source: Ref. [144]), 3D printing (Source: Ref. [145]), morphable 3D meso-structures (Source: Ref. [146]), and syringe-injectable mesh electronics (Source: Ref. [147]).

10.1002/9783527842308.ch1, Downloaded from https://onlinelibrary.wiley.com/doi/10.1002/9783527842308.ch1 by Michigan State University, Wiley Online Library on [05/09/2024]. See the Terms and Conditions (https://onlinelibrary.wiley.com/terms-and-conditions) on Wiley Online Library for rules of use; OA articles are governed by the applicable Creative Commons License

When incorporating rigid or nonstretchable electronic components into a stretchable hydrogel, the design of strong and tough interfaces between the electronic components and the hydrogel matrix becomes crucial. Figure 1.7b summarizes the recent efforts to develop strong interfacial linkages (e.g. covalent bonds [152, 153], strong physical crosslinks [154–156], and connector polymers [157, 158]) and introduce bulk dissipation mechanisms (such as viscoelasticity and Mullins effect) to create stretchable hydrogel conductors with rigid electronic components. For instance, Jin and Bao and coworkers recently proposed a method for designing a tough interface between a brittle semiconducting thin film and a stretchable substrate that effectively delayed microcrack formation in the film when stretched [143]. They achieved the tough interface using strong interfacial linkages through surface chemistry and dynamic bulk dissipations via a tough self-healing polymer matrix (TSP) that repeatedly dissipates energy via dynamic bond breakage and reformation.

In addition to interfacial design, serpentine structural design is another key feature of many stretchable hydrogel conductors with rigid or brittle electronic components. This undulating design allows the electronic components to stretch and deform together with the hydrogel matrix while minimizing the strain on the electronic components and preventing them from breaking. Figure 1.7c provides an overview of notable efforts in designing stretchable hydrogel conductors with serpentine-structured brittle electronic components. Implementing the serpentine structure design requires advanced manufacturing techniques, including micro-/nanofabrication [144, 159], 3D printing [145, 160, 161], stereographic design [146, 162, 163], and syringe injection [147, 164, 165].

1.4 Electrochemical Hydrogel Biosensors

Electrochemical biosensors have tremendous potential for medical diagnostics as they detect and measure the presence of biological molecules by converting biological events into electrical signals [166, 167]. However, previous efforts have primarily focused on graphene-based sensing materials and metallic electrodes, which have limitations when targeting *in-situ* detection. For instance, the presence of high ionic strength in body fluids produces pronounced screening of electrical fields, significantly reducing the sensitivity of the electrical chemical detection [168]. Additionally, biomarker concentrations in body fluids are typically about 10 ng/ml, which is too low to be detected by most existing electrical biosensors [169]. Recent studies show that introducing hydrogels into existing electrochemical biosensors can provide two unique benefits (Figure 1.8a) [170, 171]. First, hydrogels can act as a protective and selective layer for highly sensitive and specific *in-situ* detection, preventing interferences from biological environments (Figure 1.8b). Second, hydrogels can serve as surface modification to potentially push the limits of electrochemical properties of sensing materials, including Debye length, surface capacitance, and band gap (Figure 1.8c).

10.1002/9783527842308.ch1, Downloaded from https://onlinelibrary.wiley.com/doi/10.1002/9783527842308.ch1 by Michigan State University, Wiley Online Library on [05/09/2024]. See the Terms and Conditions (https://onlinelibrary.wiley.com/terms-and-conditions) on Wiley Online Library for rules of use; OA articles are governed by the applicable Creative Commons License

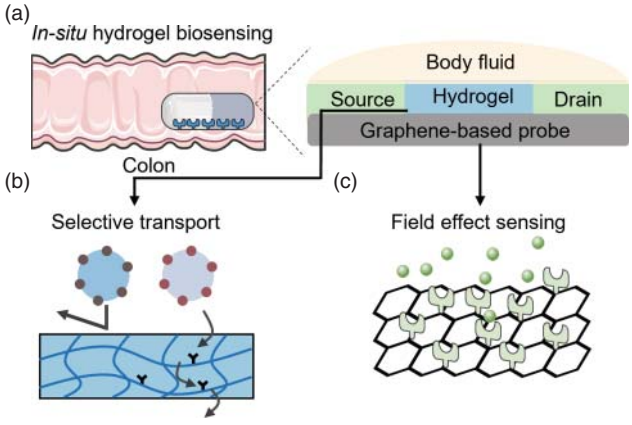


Figure 1.8 Design of electrochemical hydrogel biosensors. (a) Illustration of an electrochemical hydrogel biosensor for *in-situ* detection biomolecules. (b) Hydrogels act as a protective and selective layer for sensing materials. (c) Hydrogels serve as surface modification to potentially push the limits of electrochemical properties of sensing materials.

1.4.1 Selective Transport Design of Hydrogels

Efforts to tailor the transport properties of hydrogels mainly rely on two approaches: filtering by size (Figure 1.9a) and filtering by covalent interaction (Figure 1.9b) [172]. However, neither approach is suitable for selectively controlling the transport of biomolecules in body fluids. Filtering by size is impractical due to the small size difference between most biomolecules in body fluid; while filtering by covalent interaction is possible to distinguish the transport between target and nontarget biomolecules, such covalent interaction is only limited at the outmost surfaces of hydrogels and very challenging to achieve an enhanced transport throughout hydrogels due to the resistance from these covalent interactions. Recent studies have shown that introducing reversible interactions between target biomolecules and functional groups in hydrogels has the potential to achieve selective transport of target biomolecules across hydrogels [111, 112, 173, 174] (Figure 1.9c). The dissociation and reforming rates of the reversible interactions determine the mode and speed of biomolecular transport across hydrogels. Additionally, the network

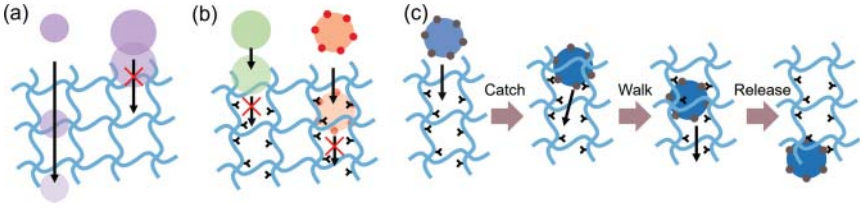


Figure 1.9 Selective transport design in hydrogels. (a) Filtering by size. (b) Filtering by permanent interaction. (c) Filtering by reversible interactions.

10.1002/9783527842308.ch1, Downloaded from https://onlinelibrary.wiley.com/doi/10.1002/9783527842308.ch1 by Michigan State University, Wiley Online Library on [05/09/2024]. See the Terms and Conditions (https://onlinelibrary.wiley.com/terms-and-conditions) on Wiley Online Library for rules of use; OA articles are governed by the applicable Creative Commons License

elasticity of hydrogels plays an important role in controlling transport. Future opportunities may focus on the synergistic role of network elasticity and reversible interaction in independently controlling the transport of various biomolecules in hydrogels. Such fundamental knowledge may also aid in understanding the selective transport mechanisms employed in biological systems, such as sperm selection by mucus layers.

1.4.2 Electrochemical Design of Hydrogel-2D Material Interfaces

The other challenge faced by *in-situ* electrochemical biosensors is their inability to detect biological events in high ionic strength solutions, ubiquitous in body fluids [166, 175]. The presence of 0.9 wt% mobile ions (Na^+, K^+, Cl^-) in body fluids leads to significant screening of electrical fields, which greatly reduces the sensitivity of electrochemical detection. For instance, the Debye length for 2D sensing materials in body fluids is typically below 1 nm, making it almost impossible to detect proteins (typically around 10 nm) above the Debye length [168]. A potential solution is to engineer the interface between the hydrogel and 2D material to enhance the field-effect sensing performance. Recent studies have shown that surface-functionalized 2D materials can achieve a 10-fold increase in Debye length from 0.82 to 9.6 nm in high ionic strength solutions [170]. One possibility is to graft crosslinked polymer networks of hydrogels onto existing sensing materials and explore the potential of optimizing the network topology and charge density in hydrogels to push the limits of electrochemical properties such as Debye length, surface capacitance, and band gap.

1.5 Flexible Hydrogel Biobattery

A flexible biobattery is a device that converts low-grade energy within the human body into usable energy and is essential for developing self-powered *in-situ* bioelectronic devices [176–179]. Hydrogels are a promising material for use in these devices because they are porous and can modulate ion and electron transport while minimizing potential leakage compared to traditional organic aqueous electrolytes. Furthermore, hydrogels are biocompatible and soft, which reduces damage to surrounding tissues. However, the power outputs of flexible hydrogel biobatteries are still relatively low and do not meet the power requirements of most *in-situ* bioelectronic devices. Figure 1.10a shows the power range and operation time requirements of common biomedical devices [180]. To develop the next generation of self-sustaining *in-situ* bioelectronic devices, high-performing hydrogels must be leveraged to harness various forms of energy within the human body (Figure 1.10b). This potential remains largely unexplored but is highly desirable. This section will discuss recent efforts in exploring the potential of powering *in-situ* bioelectronic devices through mechanical, chemical, and thermal energy harvesters (Figure 1.10c).

10.1002/9783527842308.ch1, Downloaded from https://onlinelibrary.wiley.com/doi/10.1002/9783527842308.ch1 by Michigan State University, Wiley Online Library on [05/09/2024]. See the Terms and Conditions (https://onlinelibrary.wiley.com/terms-and-conditions) on Wiley Online Library for rules of use; OA articles are governed by the applicable Creative Commons License

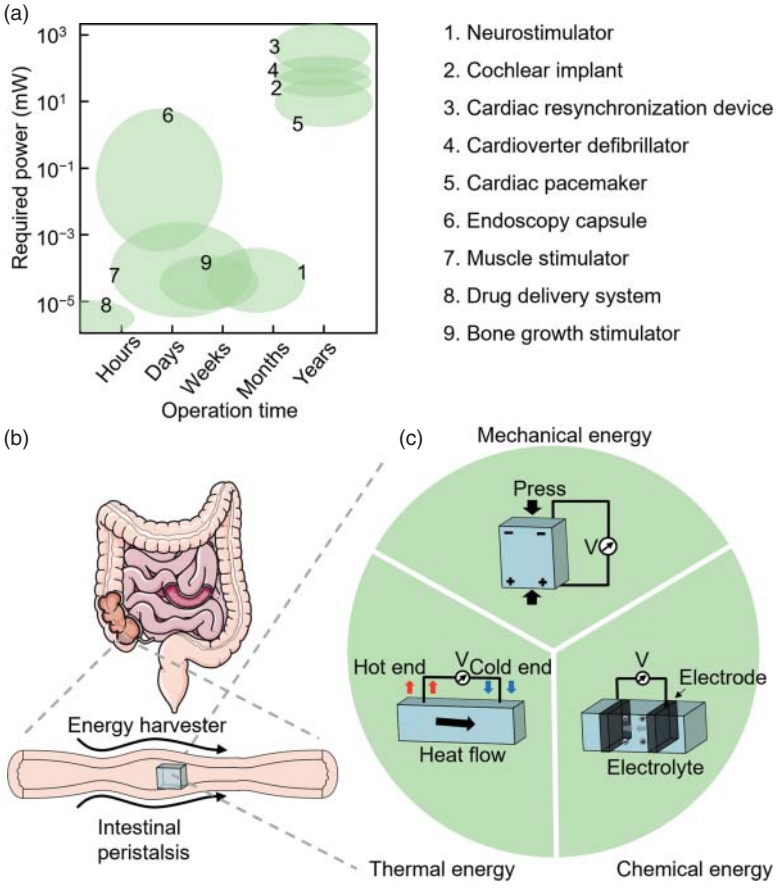


Figure 1.10 Flexible hydrogel batteries to self-power *in-situ* bioelectronic devices. (a) Examples of common implantable medical devices, with their required power supply and operation time (Source: Ref. [180]/Oxford University Press). (b) Schematic illustrations of the energy harvester working inside the intestine and (c) three forms of energy harvesting, including mechanical, chemical, and thermal energy, generated within the human body.

1.5.1 Mechanical Energy Harvester

Mechanical energy harvesters are devices that can convert the mechanical energy of the human body or organs into electrical energy for powering *in-situ* bioelectronic devices. One prime example of a mechanical energy harvester is the triboelectric nanogenerators (TENGs) [181–183], which generates an electrostatic potential difference between two materials of diverse polarities due to the triboelectric effect, causing a transfer of charges and the formation of an electric potential difference between them (Figure 1.11a) [177, 190–192]. Figure 1.11b presents a representative example of using ultrasound to induce vibrations and harness triboelectricity for in-body powering [184, 185]. Another way to harvest mechanical energy in the body is by leveraging the fluid-electro-mechanical coupling

10.1002/9783527842308.ch1, Downloaded from https://onlinelibrary.wiley.com/doi/10.1002/9783527842308.ch1 by Michigan State University, Wiley Online Library on [05/09/2024]. See the Terms and Conditions (https://onlinelibrary.wiley.com/terms-and-conditions) on Wiley Online Library for rules of use; OA articles are governed by the applicable Creative Commons License

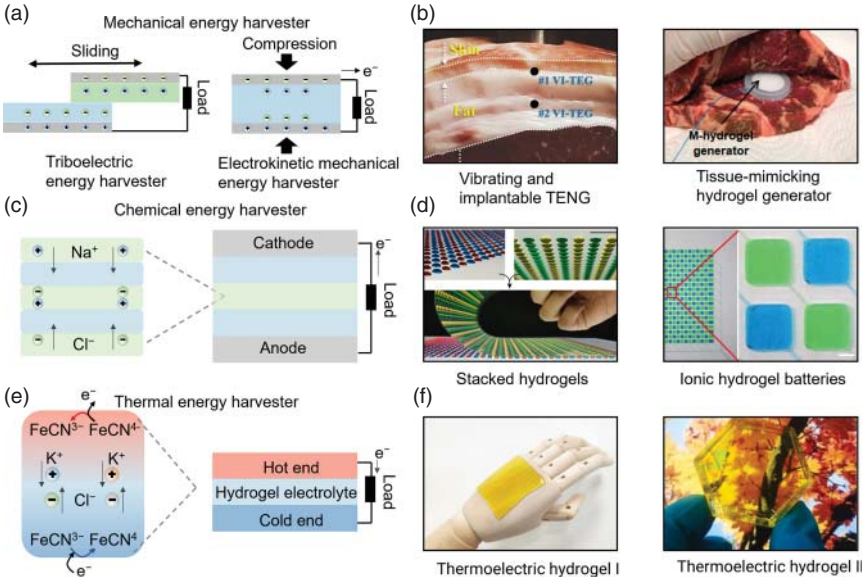


Figure 1.11 Schematic illustration of the working mechanism of (a) mechanical energy harvester with (b) examples (Source: Ref. [184] and Ref. [185]), (c) chemical energy harvester with (d) examples (Source: Ref. [186] and Ref. [187]), and (e) thermal energy harvester with (f) examples (Source: Ref. [188] and Ref. [189]. © 2022/Elsevier).

of electrokinetic streams in porous materials to generate electricity [193, 194]. Electrokinetic mechanical energy harvesters typically involve applying external forces, such as pressure, to drive the movement of micro-/nanofluidic water across a porous membrane, thereby causing the motion of ions to produce electricity. Unlike conventional TENGs, electrokinetic mechanical energy harvester can harvest low-frequency body motions while potentially producing high power output [195].

1.5.2 Chemical Energy Harvesters

Chemical energy harvesters are devices that convert chemical energy into electrical energy through chemical reactions in an electrolyte (Figure 1.11c) [196, 197]. These devices usually have two electrodes and an electrolyte, where the electrolyte acts as a mediator for the chemical reactions. The chemical reactions that occur between the positive and negative electrodes cause the flow of electrons within the electrolyte, thus generating electrical energy that can be used in the circuit. Hydrogel, with its watery nature, is an excellent carrier for chemicals, and acts as the electrolyte [198–200]. Drawing inspiration from the electric eel's power generation mechanism, Yang and Mayer and coworkers harnessed the gradients of ions in hydrogels to develop soft, flexible, transparent, and biocompatible hydrogel biobatteries, generating 110 V at open circuit or 27 mW/m^2 per hydrogel cell, which

10.1002/9783527842308.ch1, Downloaded from https://onlinelibrary.wiley.com/doi/10.1002/9783527842308.ch1 by Michigan State University, Wiley Online Library on [05/09/2024]. See the Terms and Conditions (https://onlinelibrary.wiley.com/terms-and-conditions) on Wiley Online Library for rules of use; OA articles are governed by the applicable Creative Commons License

is a significant achievement in the realm of electrochemical energy harvesting via hydrogels (Figure 1.11d) [186, 187]. Despite the abundant chemical reactions that occur within the human body (such as those that occur during digestion resulting in pH differences), there has been no significant progress in *in-situ* chemical energy harvesting. The main barriers are related to unstable ion concentrations and uncontrolled ion types in body fluids. The stability and size of the device are still the main challenges.

1.5.3 Thermal Energy Harvesters

Thermal energy harvesters using thermoelectric materials (Figure 1.11e), such as thermoelectric hydrogels, offer the potential to harvest low-grade body heat and power *in-situ* bioelectronic devices. These soft and biocompatible thermoelectric hydrogels are regarded as favorable alternatives to conventional thermoelectric materials [201–205]. Recent studies by Chen and Liu and coworkers have demonstrated a giant positive thermopower of 17 mV/K in an ionic thermoelectric hydrogel by harnessing synergistic thermo-diffusion and thermo-galvanic effects. The thermos-diffusion effect is dominated by the presence of ions (KCl, NaCl, and KNO_3), while the thermo-galvanic effect is governed by a redox couple $(Fe(CN)_6^{4-})/(Fe(CN)_6^{3-})$, also adopted in other thermoelectric hydrogels (Figure 1.11f) [188, 189]. While thermoelectric hydrogels have significant potential for *in-situ* bioelectronics, the low power output and poor mechanical properties of these materials remain key limitations. Overcoming these limitations through further research and development will be crucial to fully exploit the unique advantages of thermoelectric hydrogels in *in-situ* bioelectronics.

1.6 Concluding Remarks

Over the past few years, we have seen many exciting advances and examples in the field of *in-situ* hydrogel bioelectronics that suggest great potential of high-performing hydrogels for many important applications. We will conclude this chapter with a set of opportunities by integrating interdisciplinary efforts in various areas of *in-situ* hydrogel bioelectronics, including ingestible sensors, neural interfaces, miniature robots, and data analytics. Ingestible sensors are one area where hydrogel-based bioelectronics can be leveraged (Figure 1.12a). These sensors can be designed to be swallowed and pass through the gastrointestinal tract, allowing for noninvasive monitoring of various biomarkers in real time. With the integration of hydrogel-based sensors, these devices can provide more accurate and reliable data, as hydrogels can respond to changes in pH, temperature, and other environmental factors [32]. Neural interface technology is another area where hydrogel-based bioelectronics can be applied (Figure 1.12b) [206–209]. By using hydrogels as a platform for neural interfaces, these devices can be made more biocompatible and less invasive, reducing the risk of rejection or other complications. With the integration of hydrogel-based sensors and actuators, these

10.1002/9783527842308.ch1, Downloaded from https://onlinelibrary.wiley.com/doi/10.1002/9783527842308.ch1 by Michigan State University, Wiley Online Library on [05/09/2024]. See the Terms and Conditions (https://onlinelibrary.wiley.com/terms-and-conditions) on Wiley Online Library for rules of use; OA articles are governed by the applicable Creative Commons License

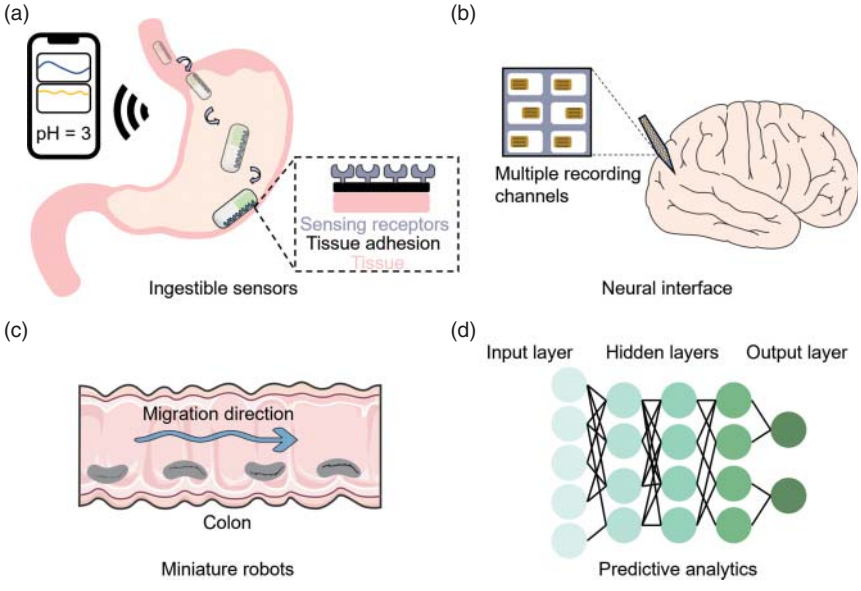


Figure 1.12 Future opportunities of *in-situ* hydrogel bioelectronics. Schematic illustrations of (a) ingestible sensors, (b) neural interfaces, (c) miniature robots, and (d) predictive analytics.

interfaces can provide more accurate and precise control over prosthetic devices or assistive technologies, allowing for more natural movements and interactions with the environment. Miniature robots are also an exciting area of research for *in-situ* hydrogel bioelectronics (Figure 1.12c) [210, 211]. With the use of hydrogels, these robots can be made more flexible and compliant, allowing for safer and more effective integration with the body. By incorporating hydrogel-based sensors and actuators, these robots can be controlled and manipulated to perform targeted drug delivery, tissue engineering, and surgical procedures. Finally, the integration of data analytics and machine learning algorithms is crucial for unlocking the full potential of *in-situ* hydrogel bioelectronics (Figure 1.12d) [212, 213]. With the vast amounts of data generated by these devices, there is a need for advanced analytics tools to help interpret and make sense of the data. By leveraging these tools, we can gain new insights into biological systems and develop more effective treatments and therapies.

Acknowledgments

We acknowledge the startup funds from the College of Engineering at Michigan State University. T. H. W is supported by financial support from the Biomedical Engineering Department at MSU.

10.1002/9783527842308.ch1, Downloaded from https://onlinelibrary.wiley.com/doi/10.1002/9783527842308.ch1 by Michigan State University, Wiley Online Library on [05/09/2024]. See the Terms and Conditions (https://onlinelibrary.wiley.com/terms-and-conditions) on Wiley Online Library for rules of use; OA articles are governed by the applicable Creative Commons License

References

1 Yu, Y., Nyein, H.Y.Y., Gao, W. et al. (2020). Flexible electrochemical bioelectronics: the rise of in situ bioanalysis. *Advanced Materials* 32 (15): 1902083.

2 Kim, D.W., Song, K.I., Seong, D. et al. (2022). Electrostatic–mechanical synergistic in situ multiscale tissue adhesion for sustainable residue-free bioelectronics interfaces. *Advanced Materials* 34 (5): 2105338.

3 Rawla, P., Sunkara, T., and Barsouk, A. (2019). Epidemiology of colorectal cancer: incidence, mortality, survival, and risk factors. *Gastroenterology Review/Przegląd Gastroenterologiczny* 14 (2): 89–103.

4 Tang, X., Shen, H., Siyuan, Z. et al. (2023). Flexible brain–computer interfaces. *Nature Electronics* 6: 1–10.

5 Zhao, S., Tang, X., Tian, W. et al. (2023). Tracking neural activity from the same cells during the entire adult life of mice. *Nature Neuroscience* 26: 1–15.

6 Steinmetz, N.A., Aydin, C., Lebedeva, A. et al. (2021). Neuropixels 2.0: a miniaturized high-density probe for stable, long-term brain recordings. *Science* 372 (6539): eabf4588.

7 Zheng, Q., Shi, B., Fan, F. et al. (2014). In vivo powering of pacemaker by breathing-driven implanted triboelectric nanogenerator. *Advanced Materials* 26 (33): 5851–5856.

8 Ryu, H., Park, H., Kim, M.K. et al. (2021). Self-rechargeable cardiac pacemaker system with triboelectric nanogenerators. *Nature Communications* 12 (1): 4374.

9 Ouyang, H., Liu, Z., Li, N. et al. (2019). Symbiotic cardiac pacemaker. *Nature Communications* 10 (1): 1–10.

10 Yuk, H., Wu, J., and Zhao, X. (2022). Hydrogel interfaces for merging humans and machines. *Nature Reviews Materials* 7 (12): 935–952.

11 Liu, X., Liu, J., Lin, S. et al. (2020). Hydrogel machines. *Materials Today* 36: 102–124.

12 Zhao, X., Chen, X., Yuk, H. et al. (2021). Soft materials by design: unconventional polymer networks give extreme properties. *Chemical Reviews* 121 (8): 4309–4372.

13 Lu, B., Yuk, H., Lin, S. et al. (2019). Pure pedot: Pss hydrogels. *Nature Communications* 10 (1): 1043.

14 Lin, X., Zhao, X., Xu, C. et al. (2022). Progress in the mechanical enhancement of hydrogels: fabrication strategies and underlying mechanisms. *Journal of Polymer Science* 60 (17): 2525–2542.

15 Kuang, X. et al. (2022). Functional tough hydrogels: design, processing, and biomedical applications. *Accounts of Materials Research* 4: 101–104.

16 Yuk, H., Lu, B., and Zhao, X. (2019). Hydrogel bioelectronics. *Chemical Society Reviews* 48 (6): 1642–1667.

17 Shi, Z., Arıcan, M.O., Zhou, T. et al. (2016). Electroconductive natural polymer-based hydrogels. *Biomaterials* 111: 40–54.

18 Lin, S., Yuk, H., Zhang, T. et al. (2016). Stretchable hydrogel electronics and devices. *Advanced Materials* 28 (22): 4497–4505.

19 Hu, L., Chee, P.L., Sugiarto, S. et al. (2022). Hydrogel-based flexible electronics. *Advanced Materials* 35: 2205326.

10.1002/9783527842308.ch1, Downloaded from https://onlinelibrary.wiley.com/doi/10.1002/9783527842308.ch1 by Michigan State University, Wiley Online Library on [05/09/2024]. See the Terms and Conditions (https://onlinelibrary.wiley.com/terms-and-conditions) on Wiley Online Library for rules of use; OA articles are governed by the applicable Creative Commons License

20 Guo, X., Li, J., Wang, F. et al. (2022). Application of conductive polymer hydrogels in flexible electronics. *Journal of Polymer Science* 60 (18): 2635–2662.

21 Gong, J.P., Katsuyama, Y., Kurokawa, T. et al. (2003). Double-network hydrogels with extremely high mechanical strength. *Advanced Materials* 15 (14): 1155–1158.

22 Sun, T.L., Kurokawa, T., Kuroda, S. et al. (2013). Physical hydrogels composed of polyampholytes demonstrate high toughness and viscoelasticity. *Nature Materials* 12 (10): 932–937.

23 Sun, J.-Y., Zhao, X., Illeperuma, W.R.K. et al. (2012). Highly stretchable and tough hydrogels. *Nature* 489 (7414): 133–136.

24 Yang, J., Bai, R., Chen, B. et al. (2020). Hydrogel adhesion: a supramolecular synergy of chemistry, topology, and mechanics. *Advanced Functional Materials* 30 (2): 1901693.

25 Yang, H., Li, C., Tang, J. et al. (2019). Strong and degradable adhesion of hydrogels. *ACS Applied Bio Materials* 2 (5): 1781–1786.

26 Steck, J., Yang, J., and Suo, Z. (2019). Covalent topological adhesion. *ACS Macro Letters* 8 (6): 754–758.

27 Yuk, H., Zhang, T., Lin, S. et al. (2016). Tough bonding of hydrogels to diverse non-porous surfaces. *Nature Materials* 15 (2): 190–196.

28 Liu, J., Lin, S., Liu, X. et al. (2020). Fatigue-resistant adhesion of hydrogels. *Nature Communications* 11 (1): 1071.

29 Li, J., Celiz, A.D., Yang, J. et al. (2017). Tough adhesives for diverse wet surfaces. *Science* 357 (6349): 378–381.

30 Wirthl, D., Pichler, R., Drack, M. et al. (2017). Instant tough bonding of hydrogels for soft machines and electronics. *Science Advances* 3 (6): e1700053.

31 Deng, J., Yuk, H., Wu, J. et al. (2021). Electrical bioadhesive interface for bioelectronics. *Nature Materials* 20 (2): 229–236.

32 Liu, X., Steiger, C., Lin, S. et al. (2019). Ingestible hydrogel device. *Nature Communications* 10 (1): 493.

33 Li, S., Cong, Y., and Fu, J. (2021). Tissue adhesive hydrogel bioelectronics. *Journal of Materials Chemistry B* 9 (22): 4423–4443.

34 Xie, C., Wang, X., He, H. et al. (2020). Mussel-inspired hydrogels for self-adhesive bioelectronics. *Advanced Functional Materials* 30 (25): 1909954.

35 Jia, M. and Rolandi, M. (2020). Soft and ion-conducting materials in bioelectronics: from conducting polymers to hydrogels. *Advanced Healthcare Materials* 9 (5): 1901372.

36 Dechiraju, H., Jia, M., Luo, L. et al. (2022). Ion-conducting hydrogels and their applications in bioelectronics. *Advanced Sustainable Systems* 6 (2): 2100173.

37 Yu, Q., Zheng, Z., Dong, X. et al. (2021). Mussel-inspired hydrogels as tough, self-adhesive and conductive bioelectronics: a review. *Soft Matter* 17 (39): 8786–8804.

38 Storm, C., Pastore, J.J., MacKintosh, F.C. et al. (2005). Nonlinear elasticity in biological gels. *Nature* 435 (7039): 191–194.

39 Ganji, F., Vasheghani, F.S., and Vasheghani, F.E. (2010). Theoretical description of hydrogel swelling: a review. *Iranian Polymer Journal* 19 (5): 375–398.

10.1002/9783527842308.ch1, Downloaded from https://onlinelibrary.wiley.com/doi/10.1002/9783527842308.ch1 by Michigan State University, Wiley Online Library on [05/09/2024]. See the Terms and Conditions (https://onlinelibrary.wiley.com/terms-and-conditions) on Wiley Online Library for rules of use; OA articles are governed by the applicable Creative Commons License

40 Kim, S.W., Bae, Y.H., and Okano, T. (1992). Hydrogels: swelling, drug loading, and release. *Pharmaceutical Research* 9: 283–290.

41 Holback, H., Yeo, Y., and Park, K. (2011). Hydrogel swelling behavior and its biomedical applications. In: *Biomedical Hydrogels* (ed. S. Rimmer), 3–24. Elsevier.

42 Chen, J., Park, H., and Park, K. (1999). Synthesis of superporous hydrogels: hydrogels with fast swelling and superabsorbent properties. *Journal of Biomedical Materials Research: An Official Journal of The Society for Biomaterials, The Japanese Society for Biomaterials, and the Australian Society for Biomaterials* 44 (1): 53–62.

43 Canal, T. and Peppas, N.A. (1989). Correlation between mesh size and equilibrium degree of swelling of polymeric networks. *Journal of Biomedical Materials Research* 23 (10): 1183–1193.

44 Hong, W., Zhao, X., Zhou, J. et al. (2008). A theory of coupled diffusion and large deformation in polymeric gels. *Journal of the Mechanics and Physics of Solids* 56 (5): 1779–1793.

45 Chester, S.A. and Anand, L. (2010). A coupled theory of fluid permeation and large deformations for elastomeric materials. *Journal of the Mechanics and Physics of Solids* 58 (11): 1879–1906.

46 Zhao, X., Huebsch, N., Mooney, D.J. et al. (2010). Stress-relaxation behavior in gels with ionic and covalent crosslinks. *Journal of Applied Physics* 107 (6): 063509.

47 Long, R., Mayumi, K., Creton, C. et al. (2014). Time dependent behavior of a dual cross-link self-healing gel: theory and experiments. *Macromolecules* 47 (20): 7243–7250.

48 Guo, J., Long, R., Mayumi, K. et al. (2016). Mechanics of a dual cross-link gel with dynamic bonds: steady state kinetics and large deformation effects. *Macromolecules* 49 (9): 3497–3507.

49 Mao, Y., Lin, S., Zhao, X. et al. (2017). A large deformation viscoelastic model for double-network hydrogels. *Journal of the Mechanics and Physics of Solids* 100: 103–130.

50 Grindy, S.C., Learsch, R., Mozhdehi, D. et al. (2015). Control of hierarchical polymer mechanics with bioinspired metal-coordination dynamics. *Nature Materials* 14 (12): 1210–1216.

51 Zhang, T., Lin, S., Yuk, H. et al. (2015). Predicting fracture energies and crack-tip fields of soft tough materials. *Extreme Mechanics Letters* 4: 1–8.

52 Qi, Y., Caillard, J., and Long, R. (2018). Fracture toughness of soft materials with rate-independent hysteresis. *Journal of the Mechanics and Physics of Solids* 118: 341–364.

53 Long, R. and Hui, C.-Y. (2016). Fracture toughness of hydrogels: measurement and interpretation. *Soft Matter* 12 (39): 8069–8086.

54 Bai, R., Yang, Q., Tang, J. et al. (2017). Fatigue fracture of tough hydrogels. *Extreme Mechanics Letters* 15: 91–96.

55 Bai, R., Yang, J., and Suo, Z. (2019). Fatigue of hydrogels. *European Journal of Mechanics-A/Solids* 74: 337–370.

10.1002/9783527842308.ch1, Downloaded from https://onlinelibrary.wiley.com/doi/10.1002/9783527842308.ch1 by Michigan State University, Wiley Online Library on [05/09/2024]. See the Terms and Conditions (https://onlinelibrary.wiley.com/terms-and-conditions) on Wiley Online Library for rules of use; OA articles are governed by the applicable Creative Commons License

56 Lin, S., Liu, X., Liu, J. et al. (2019). Anti-fatigue-fracture hydrogels. *Science Advances* 5 (1): eaau8528.

57 Li, X., Cui, K., Sun, T.L. et al. (2020). Mesoscale bicontinuous networks in self-healing hydrogels delay fatigue fracture. *Proceedings of the National Academy of Sciences* 117 (14): 7606–7612.

58 Lake, G. and Lindley, P. (1965). The mechanical fatigue limit for rubber. *Journal of Applied Polymer Science* 9 (4): 1233–1251.

59 Biot, M.A. (1941). General theory of three-dimensional consolidation. *Journal of Applied Physics* 12 (2): 155–164.

60 Flory, P.J. (1953). *Principles of Polymer Chemistry*. Cornell University Press.

61 Lake, G. and Thomas, A. (1967). The strength of highly elastic materials. *Proceedings of the Royal Society of London. Series A. Mathematical and Physical Sciences* 300 (1460): 108–119.

62 Treloar, L.G. (1975). *The Physics of Rubber Elasticity*. OUP Oxford.

63 De Gennes, P.-G. and Gennes, P.-G. (1979). *Scaling Concepts in Polymer Physics*. Cornell University Press.

64 Gent, A.N. (1996). A new constitutive relation for rubber. *Rubber Chemistry and Technology* 69 (1): 59–61.

65 Boyce, M.C. and Arruda, E.M. (2000). Constitutive models of rubber elasticity: a review. *Rubber Chemistry and Technology* 73 (3): 504–523.

66 Rubinstein, M. and Colby, R.H. (2003). *Polymer Physics*, vol. 23. New York: Oxford University Press.

67 Mark, J.E. and Erman, B. (2007). *Rubberlike Elasticity: A Molecular Primer*. Cambridge University Press.

68 Argon, A.S. (2013). *The Physics of Deformation and Fracture of Polymers*. Cambridge: New York.

69 Creton, C. and Ciccotti, M. (2016). Fracture and adhesion of soft materials: a review. *Reports on Progress in Physics* 79 (4): 046601.

70 Lin, S., Mao, Y., Radovitzky, R. et al. (2017). Instabilities in confined elastic layers under tension: fringe, fingering and cavitation. *Journal of the Mechanics and Physics of Solids* 106: 229–256.

71 Baby, D.K. (2020). Rheology of hydrogels. In: *Rheology of Polymer Blends and Nanocomposites* (ed. S. Thomas, C. Sarathchandran, and N. Chandran), 193–204. Elsevier.

72 Hu, Y., Zhao, X., Vlassak, J.J. et al. (2010). Using indentation to characterize the poroelasticity of gels. *Applied Physics Letters* 96 (12): 121904.

73 Zhong, M., Wang, R., Kawamoto, K. et al. (2016). Quantifying the impact of molecular defects on polymer network elasticity. *Science* 353 (6305): 1264–1268.

74 Gu, Y., Zhao, J., and Johnson, J.A. (2019). A (macro) molecular-level understanding of polymer network topology. *Trends in Chemistry* 1 (3): 318–334.

75 Rivlin, R. and Thomas, A.G. (1953). Rupture of rubber. I. Characteristic energy for tearing. *Journal of Polymer Science* 10 (3): 291–318.

76 Wang, Y., Yin, T., and Suo, Z. (2021). Polyacrylamide hydrogels. III. Lap shear and peel. *Journal of the Mechanics and Physics of Solids* 150: 104348.

77 Bai, R., Chen, B., Yang, J. et al. (2019). Tearing a hydrogel of complex rheology. *Journal of the Mechanics and Physics of Solids* 125: 749–761.

10.1002/9783527842308.ch1, Downloaded from https://onlinelibrary.wiley.com/doi/10.1002/9783527842308.ch1 by Michigan State University, Wiley Online Library on [05/09/2024]. See the Terms and Conditions (https://onlinelibrary.wiley.com/terms-and-conditions) on Wiley Online Library for rules of use; OA articles are governed by the applicable Creative Commons License

78 Zhao, X. (2014). Multi-scale multi-mechanism design of tough hydrogels: building dissipation into stretchy networks. *Soft Matter* 10 (5): 672–687.

79 Tang, J., Li, J., Vlassak, J.J. et al. (2017). Fatigue fracture of hydrogels. *Extreme Mechanics Letters* 10: 24–31.

80 Lin, S. and Zhao, X. (2020). Fracture of polymer networks with diverse topological defects. *Physical Review E* 102 (5): 052503.

81 James, H.M. and Guth, E. (1943). Theory of the elastic properties of rubber. *The Journal of Chemical Physics* 11 (10): 455–481.

82 Cao, J., Li, J., Chen, Y. et al. (2018). Dual physical crosslinking strategy to construct moldable hydrogels with ultrahigh strength and toughness. *Advanced Functional Materials* 28 (23): 1800739.

83 Hu, Z. and Chen, G. (2014). Novel nanocomposite hydrogels consisting of layered double hydroxide with ultrahigh tensibility and hierarchical porous structure at low inorganic content. *Advanced Materials* 26 (34): 5950–5956.

84 Tsukeshiba, H., Huang, M., Na, Y.H. et al. (2005). Effect of polymer entanglement on the toughening of double network hydrogels. *The Journal of Physical Chemistry B* 109 (34): 16304–16309.

85 Gong, J.P. (2010). Why are double network hydrogels so tough? *Soft Matter* 6 (12): 2583–2590.

86 de Gennes, P.-G. (1996). Soft adhesives. *Langmuir* 12 (19): 4497–4500.

87 Chen, Q. et al. (2016). Engineering of tough double network hydrogels. *Macromolecular Chemistry and Physics* 217 (9): 1022–1036.

88 Li, J., Suo, Z., and Vlassak, J.J. (2014). Stiff, strong, and tough hydrogels with good chemical stability. *Journal of Materials Chemistry B* 2 (39): 6708–6713.

89 Wang, Z., Zheng, X., Ouchi, T. et al. (2021). Toughening hydrogels through force-triggered chemical reactions that lengthen polymer strands. *Science* 374 (6564): 193–196.

90 Luo, F., Sun, T.L., Nakajima, T. et al. (2014). Crack blunting and advancing behaviors of tough and self-healing polyampholyte hydrogel. *Macromolecules* 47 (17): 6037–6046.

91 Haque, M.A., Kurokawa, T., and Gong, J.P. (2012). Super tough double network hydrogels and their application as biomaterials. *Polymer* 53 (9): 1805–1822.

92 Chen, C., Wang, Z., and Suo, Z. (2017). Flaw sensitivity of highly stretchable materials. *Extreme Mechanics Letters* 10: 50–57.

93 Lin, S., Londono, C.D., Zheng, D. et al. (2022). An extreme toughening mechanism for soft materials. *Soft Matter* 18 (31): 5742–5749.

94 Sun, T.L., Londono, C.D., Zheng, D. et al. (2017). Bulk energy dissipation mechanism for the fracture of tough and self-healing hydrogels. *Macromolecules* 50 (7): 2923–2931.

95 Liu, C., Morimoto, N., Jiang, L. et al. (2021). Tough hydrogels with rapid self-reinforcement. *Science* 372 (6546): 1078–1081.

96 Kim, J., Zhang, G., Shi, M. et al. (2021). Fracture, fatigue, and friction of polymers in which entanglements greatly outnumber cross-links. *Science* 374 (6564): 212–216.

10.1002/9783527842308.ch1, Downloaded from https://onlinelibrary.wiley.com/doi/10.1002/9783527842308.ch1 by Michigan State University, Wiley Online Library on [05/09/2024]. See the Terms and Conditions (https://onlinelibrary.wiley.com/terms-and-conditions) on Wiley Online Library for rules of use; OA articles are governed by the applicable Creative Commons License

97 Zheng, D., Lin, S., Ni, J. et al. (2022). Fracture and fatigue of entangled and unentangled polymer networks. *Extreme Mechanics Letters* 51: 101608.

98 Norioka, C., Inamoto, Y., Hajime, C. et al. (2021). A universal method to easily design tough and stretchable hydrogels. *NPG Asia Materials* 13 (1): 34.

99 Zhang, E., Bai, R., Morelle, X.P. et al. (2018). Fatigue fracture of nearly elastic hydrogels. *Soft Matter* 14 (18): 3563–3571.

100 Lin, S., Liu, J., Liu, X. et al. (2019). Muscle-like fatigue-resistant hydrogels by mechanical training. *Proceedings of the National Academy of Sciences* 116 (21): 10244–10249.

101 Bai, R., Yang, J., Morelle, X.P. et al. (2018). Fatigue fracture of self-recovery hydrogels. *ACS Macro Letters* 7 (3): 312–317.

102 Liang, X., Chen, G., Lin, S. et al. (2022). Bioinspired 2D isotropically fatigue-resistant hydrogels. *Advanced Materials* 34 (8): 2107106.

103 Hua, M., Wu, S., Ma, Y. et al. (2021). Strong tough hydrogels via the synergy of freeze-casting and salting out. *Nature* 590 (7847): 594–599.

104 Guo, X., Dong, X., Zou, G. et al. (2023). Strong and tough fibrous hydrogels reinforced by multiscale hierarchical structures with multimechanisms. *Science Advances* 9 (2): eadf7075.

105 Ni, J., Lin, S., Qin, Z. et al. (2021). Strong fatigue-resistant nanofibrous hydrogels inspired by lobster underbelly. *Matter* 4 (6): 1919–1934.

106 Xiang, C., Wang, Z., Yang, C. et al. (2020). Stretchable and fatigue-resistant materials. *Materials Today* 34: 7–16.

107 Li, X., Cui, K., Kurokawa, T. et al. (2021). Effect of mesoscale phase contrast on fatigue-delaying behavior of self-healing hydrogels. *Science Advances* 7 (16): eabe8210.

108 Edward, J.T. (1970). Molecular volumes and the Stokes-Einstein equation. *Journal of Chemical Education* 47 (4): 261.

109 Moncure, P.J., Simon, Z.C., Millstone, J.E. et al. (2022). Relationship between gel mesh and particle size in determining nanoparticle diffusion in hydrogel nanocomposites. *The Journal of Physical Chemistry B* 126 (22): 4132–4142.

110 Cai, L.-H., Panyukov, S., and Rubinstein, M. (2015). Hopping diffusion of nanoparticles in polymer matrices. *Macromolecules* 48 (3): 847–862.

111 Yang, Y.J., Mai, D.J., Dursch, T.J. et al. (2018). Nucleopore-inspired polymer hydrogels for selective biomolecular transport. *Biomacromolecules* 19 (10): 3905–3916.

112 Gu, Y., Distler, M.E., Cheng, H.F. et al. (2021). A general DNA-gated hydrogel strategy for selective transport of chemical and biological cargos. *Journal of the American Chemical Society* 143 (41): 17200–17208.

113 Maguire, L., Stefferson, M., Betterton, M.D. et al. (2019). Design principles of selective transport through biopolymer barriers. *Physical Review E* 100 (4): 042414.

114 Cheng, T., Zhang, Y.Z., Wang, S. et al. (2021). Conductive hydrogel-based electrodes and electrolytes for stretchable and self-healable supercapacitors. *Advanced Functional Materials* 31 (24): 2101303.

10.1002/9783527842308.ch1, Downloaded from https://onlinelibrary.wiley.com/doi/10.1002/9783527842308.ch1 by Michigan State University, Wiley Online Library on [05/09/2024]. See the Terms and Conditions (https://onlinelibrary.wiley.com/terms-and-conditions) on Wiley Online Library for rules of use; OA articles are governed by the applicable Creative Commons License

115 Deng, Z., Yu, R., and Guo, B. (2021). Stimuli-responsive conductive hydrogels: design, properties, and applications. *Materials Chemistry Frontiers* 5 (5): 2092–2123.

116 Shen, Z., Zhang, Z., Zhang, N. et al. (2022). High-stretchability, ultralow-hysteresis conducting polymer hydrogel strain sensors for soft machines. *Advanced Materials* 34 (32): 2203650.

117 Fu, F., Wang, J., Zeng, H. et al. (2020). Functional conductive hydrogels for bioelectronics. *ACS Materials Letters* 2 (10): 1287–1301.

118 Huang, H., Han, L., Li, J. et al. (2020). Super-stretchable, elastic and recoverable ionic conductive hydrogel for wireless wearable, stretchable sensor. *Journal of Materials Chemistry A* 8 (20): 10291–10300.

119 Huang, H., Han, L., Fu, X. et al. (2020). Multiple stimuli responsive and identifiable zwitterionic ionic conductive hydrogel for bionic electronic skin. *Advanced Electronic Materials* 6 (7): 2000239.

120 Shi, Y., Ma, C., Peng, L. et al. (2015). Conductive "smart" hybrid hydrogels with PNIPAM and nanostructured conductive polymers. *Advanced Functional Materials* 25 (8): 1219–1225.

121 Mondal, S., Das, S., and Nandi, A.K. (2020). A review on recent advances in polymer and peptide hydrogels. *Soft Matter* 16 (6): 1404–1454.

122 Zhang, C., Wang, M., Jiang, C. et al. (2022). Highly adhesive and self-healing γ-PGA/PEDOT: PSS conductive hydrogels enabled by multiple hydrogen bonding for wearable electronics. *Nano Energy* 95: 106991.

123 Shi, J., Chen, X., Li, G. et al. (2019). A liquid PEDOT: PSS electrode-based stretchable triboelectric nanogenerator for a portable self-charging power source. *Nanoscale* 11 (15): 7513–7519.

124 Guzinski, M., Jarvis, J.M., Perez, F. et al. (2017). PEDOT (PSS) as solid contact for ion-selective electrodes: the influence of the PEDOT (PSS) film thickness on the equilibration times. *Analytical Chemistry* 89 (6): 3508–3516.

125 Sun, X., Yao, F., and Li, J. (2020). Nanocomposite hydrogel-based strain and pressure sensors: a review. *Journal of Materials Chemistry A* 8 (36): 18605–18623.

126 Han, L., Yan, L., Wang, M. et al. (2018). Transparent, adhesive, and conductive hydrogel for soft bioelectronics based on light-transmitting polydopamine-doped polypyrrole nanofibrils. *Chemistry of Materials* 30 (16): 5561–5572.

127 Ohm, Y., Liao, J., Luo, Y. et al. (2022). Reconfigurable electrical networks within a conductive hydrogel composite. *Advanced Materials* 35: 2209408.

128 Hui, Y., Yao, Y., Qian, Q. et al. (2022). Three-dimensional printing of soft hydrogel electronics. *Nature Electronics* 5: 1–11.

129 Yasuda, K., Gong, J.P., Katsuyama, Y. et al. (2005). Biomechanical properties of high-toughness double network hydrogels. *Biomaterials* 26 (21): 4468–4475.

130 Kong, H.J., Wong, E., and Mooney, D.J. (2003). Independent control of rigidity and toughness of polymeric hydrogels. *Macromolecules* 36 (12): 4582–4588.

131 Tuncaboylu, D.C., Sari, M., Oppermann, W. et al. (2011). Tough and self-healing hydrogels formed via hydrophobic interactions. *Macromolecules* 44 (12): 4997–5005.

10.1002/9783527842308.ch1, Downloaded from https://onlinelibrary.wiley.com/doi/10.1002/9783527842308.ch1 by Michigan State University, Wiley Online Library on [05/09/2024]. See the Terms and Conditions (https://onlinelibrary.wiley.com/terms-and-conditions) on Wiley Online Library for rules of use; OA articles are governed by the applicable Creative Commons License

132 Abdurrahmanoglu, S., Can, V., and Okay, O. (2009). Design of high-toughness polyacrylamide hydrogels by hydrophobic modification. *Polymer* 50 (23): 5449–5455.

133 Seitz, M.E., Martina, D., Baumberger, T. et al. (2009). Fracture and large strain behavior of self-assembled triblock copolymer gels. *Soft Matter* 5 (2): 447–456.

134 Haraguchi, K. and Takehisa, T. (2002). Nanocomposite hydrogels: a unique organic–inorganic network structure with extraordinary mechanical, optical, and swelling/de-swelling properties. *Advanced Materials* 14 (16): 1120–1124.

135 Haraguchi, K. and Li, H.J. (2005). Control of the coil-to-globule transition and ultrahigh mechanical properties of PNIPA in nanocomposite hydrogels. *Angewandte Chemie International Edition* 44 (40): 6500–6504.

136 Sakai, T., Matsunaga, T., Yamamoto, Y. et al. (2008). Design and fabrication of a high-strength hydrogel with ideally homogeneous network structure from tetrahedron-like macromonomers. *Macromolecules* 41 (14): 5379–5384.

137 Sakai, T., Akagi, Y., Matsunaga, T. et al. (2010). Highly elastic and deformable hydrogel formed from tetra-arm polymers. *Macromolecular Rapid Communications* 31 (22): 1954–1959.

138 Liao, I.C., Moutos, F.T., Estes, B.T. et al. (2013). Composite three-dimensional woven scaffolds with interpenetrating network hydrogels to create functional synthetic articular cartilage. *Advanced Functional Materials* 23 (47): 5833–5839.

139 Lin, S., Cao, C., Wang, Q. et al. (2014). Design of stiff, tough and stretchy hydrogel composites via nanoscale hybrid crosslinking and macroscale fiber reinforcement. *Soft Matter* 10 (38): 7519–7527.

140 King, D.R., Sun, T.L., Huang, Y. et al. (2015). Extremely tough composites from fabric reinforced polyampholyte hydrogels. *Materials Horizons* 2 (6): 584–591.

141 Nezakati, T., Seifalian, A., Tan, A. et al. (2018). Conductive polymers: opportunities and challenges in biomedical applications. *Chemical Reviews* 118 (14): 6766–6843.

142 Feig, V.R., Tran, H., Lee, M. et al. (2018). Mechanically tunable conductive interpenetrating network hydrogels that mimic the elastic moduli of biological tissue. *Nature Communications* 9 (1): 2740.

143 Kang, J., Mun, J., Zheng, Y. et al. (2022). Tough-interface-enabled stretchable electronics using non-stretchable polymer semiconductors and conductors. *Nature Nanotechnology* 17: 1–7.

144 Han, M., Chen, L., Aras, K. et al. (2020). Catheter-integrated soft multilayer electronic arrays for multiplexed sensing and actuation during cardiac surgery. *Nature Biomedical Engineering* 4 (10): 997–1009.

145 Asulin, M., Michael, I., Shapira, A. et al. (2021). One-step 3D printing of heart patches with built-in electronics for performance regulation. *Advanced Science* 8 (9): 2004205.

146 Yan, Z., Zhang, F., Liu, F. et al. (2016). Mechanical assembly of complex, 3D mesostructures from releasable multilayers of advanced materials. *Science Advances* 2 (9): e1601014.

147 Hong, G., Yang, X., Zhou, T. et al. (2018). Mesh electronics: a new paradigm for tissue-like brain probes. *Current Opinion in Neurobiology* 50: 33–41.

10.1002/9783527842308.ch1, Downloaded from https://onlinelibrary.wiley.com/doi/10.1002/9783527842308.ch1 by Michigan State University, Wiley Online Library on [05/09/2024]. See the Terms and Conditions (https://onlinelibrary.wiley.com/terms-and-conditions) on Wiley Online Library for rules of use; OA articles are governed by the applicable Creative Commons License

148 Choi, S., Han, S.I., Kim, D. et al. (2019). High-performance stretchable conductive nanocomposites: materials, processes, and device applications. *Chemical Society Reviews* 48 (6): 1566–1595.

149 Yuk, H., Lu, B., Lin, S. et al. (2020). 3D printing of conducting polymers. *Nature Communications* 11 (1): 1604.

150 Vallem, V., Roosa, E., Ledinh, T. et al. (2021). A soft variable-area electrical-double-layer energy harvester. *Advanced Materials* 33 (43): 2103142.

151 Shay, T., Velev, O.D., and Dickey, M.D. (2018). Soft electrodes combining hydrogel and liquid metal. *Soft Matter* 14 (17): 3296–3303.

152 Mao, S., Zhang, D., Zhang, Y. et al. (2020). A universal coating strategy for controllable functionalized polymer surfaces. *Advanced Functional Materials* 30 (40): 2004633.

153 Wei, K., Chen, X., Zhao, P. et al. (2019). Stretchable and bioadhesive supramolecular hydrogels activated by a one-stone–two-bird postgelation functionalization method. *ACS Applied Materials & Interfaces* 11 (18): 16328–16335.

154 Liu, Q., Nian, G., Yang, C. et al. (2018). Bonding dissimilar polymer networks in various manufacturing processes. *Nature Communications* 9 (1): 846.

155 Chen, H., Liu, Y., Ren, B. et al. (2017). Super bulk and interfacial toughness of physically crosslinked double-network hydrogels. *Advanced Functional Materials* 27 (44): 1703086.

156 Fan, H., Wang, J., Tao, Z. et al. (2019). Adjacent cationic–aromatic sequences yield strong electrostatic adhesion of hydrogels in seawater. *Nature Communications* 10 (1): 5127.

157 Ji, H. and De Gennes, P. (1993). Adhesion via connector molecules: the many-stitch problem. *Macromolecules* 26 (3): 520–525.

158 Raphael, E. and De Gennes, P. (1992). Rubber-rubber adhesion with connector molecules. *The Journal of Physical Chemistry* 96 (10): 4002–4007.

159 Wong, T.H., Liu, Y., Li, J. et al. (2021). Triboelectric nanogenerator tattoos enabled by epidermal electronic technologies. *Advanced Functional Materials* 32: 2111269.

160 Kamyshny, A. and Magdassi, S. (2019). Conductive nanomaterials for 2D and 3D printed flexible electronics. *Chemical Society Reviews* 48 (6): 1712–1740.

161 Shin, S.R., Farzad, M.R., Tamayol, A. et al. (2016). A bioactive carbon nanotube-based ink for printing 2D and 3D flexible electronics. *Advanced Materials* 28 (17): 3280–3289.

162 Cheng, X. and Zhang, Y. (2019). Micro/nanoscale 3D assembly by rolling, folding, curving, and buckling approaches. *Advanced Materials* 31 (36): 1901895.

163 Zhao, H., Kim, Y., Wang, H. et al. (2021). Compliant 3D frameworks instrumented with strain sensors for characterization of millimeter-scale engineered muscle tissues. *Proceedings of the National Academy of Sciences* 118 (19): e2100077118.

164 Liu, J. (2018). Syringe injectable electronics. In: *Biomimetics Through Nanoelectronics* (ed. J. Liu), 65–93. Springer.

165 Dai, X. et al. (2018). Mesh nanoelectronics: seamless integration of electronics with tissues. *Accounts of Chemical Research* 51 (2): 309–318.

10.1002/9783527842308.ch1, Downloaded from https://onlinelibrary.wiley.com/doi/10.1002/9783527842308.ch1 by Michigan State University, Wiley Online Library on [05/09/2024]. See the Terms and Conditions (https://onlinelibrary.wiley.com/terms-and-conditions) on Wiley Online Library for rules of use; OA articles are governed by the applicable Creative Commons License

166 Ronkainen, N.J., Halsall, H.B., and Heineman, W.R. (2010). Electrochemical biosensors. *Chemical Society Reviews* 39 (5): 1747–1763.

167 Mahshid, S.S., Flynn, S.E., and Mahshid, S. (2021). The potential application of electrochemical biosensors in the COVID-19 pandemic: a perspective on the rapid diagnostics of SARS-CoV-2. *Biosensors and Bioelectronics* 176: 112905.

168 Kesler, V., Murmann, B., and Soh, H.T. (2020). Going beyond the debye length: overcoming charge screening limitations in next-generation bioelectronic sensors. *ACS Nano* 14 (12): 16194–16201.

169 Menon, S., Mathew, M.R., Sam, S. et al. (2020). Recent advances and challenges in electrochemical biosensors for emerging and re-emerging infectious diseases. *Journal of Electroanalytical Chemistry* 878: 114596.

170 Piccinini, E., Alberti, S., Longo, G.S. et al. (2018). Pushing the boundaries of interfacial sensitivity in graphene FET sensors: polyelectrolyte multilayers strongly increase the Debye screening length. *The Journal of Physical Chemistry C* 122 (18): 10181–10188.

171 Gao, N., Gao, T., Yang, X. et al. (2016). Specific detection of biomolecules in physiological solutions using graphene transistor biosensors. *Proceedings of the National Academy of Sciences* 113 (51): 14633–14638.

172 Lieleg, O. and Ribbeck, K. (2011). Biological hydrogels as selective diffusion barriers. *Trends in Cell Biology* 21 (9): 543–551.

173 Kim, M., Chen, W.G., Kang, J.W. et al. (2015). Artificially engineered protein hydrogels adapted from the nucleoporin Nsp1 for selective biomolecular transport. *Advanced Materials* 27 (28): 4207–4212.

174 Yang, Y.J., Mai, D.J., Li, S. et al. (2021). Tuning selective transport of biomolecules through site-mutated nucleoporin-like protein (NLP) hydrogels. *Biomacromolecules* 22 (2): 289–298.

175 Purwidyantri, A., Domingues, T., Borme, J. et al. (2021). Influence of the electrolyte salt concentration on DNA detection with graphene transistors. *Biosensors* 11 (1): 24.

176 Kishore, R.A. and Priya, S. (2018). A review on low-grade thermal energy harvesting: materials, methods and devices. *Materials* 11 (8): 1433.

177 Fan, F.-R., Tian, Z.-Q., and Wang, Z.L. (2012). Flexible triboelectric generator. *Nano Energy* 1 (2): 328–334.

178 Zhu, G., Pan, C., Guo, W. et al. (2012). Triboelectric-generator-driven pulse electrodeposition for micropatterning. *Nano Letters* 12 (9): 4960–4965.

179 Kim, S., Choi, S.J., Zhao, K. et al. (2016). Electrochemically driven mechanical energy harvesting. *Nature Communications* 7 (1): 10146.

180 Stauss, S. and Honma, I. (2018). Biocompatible batteries—materials and chemistry, fabrication, applications, and future prospects. *Bulletin of the Chemical Society of Japan* 91 (3): 492–505.

181 Zheng, Q., Shi, B., Li, Z. et al. (2017). Recent progress on piezoelectric and triboelectric energy harvesters in biomedical systems. *Advanced Science* 4 (7): 1700029.

182 Song, Y., Shi, Z., Hu, G.H. et al. (2021). Recent advances in cellulose-based piezoelectric and triboelectric nanogenerators for energy harvesting: a review. *Journal of Materials Chemistry A* 9 (4): 1910–1937.

10.1002/9783527842308.ch1, Downloaded from https://onlinelibrary.wiley.com/doi/10.1002/9783527842308.ch1 by Michigan State University, Wiley Online Library on [05/09/2024]. See the Terms and Conditions (https://onlinelibrary.wiley.com/terms-and-conditions) on Wiley Online Library for rules of use; OA articles are governed by the applicable Creative Commons License

183 Luo, J. and Wang, Z.L. (2020). Recent progress of triboelectric nanogenerators: from fundamental theory to practical applications. *EcoMat* 2 (4): e12059.

184 Hinchet, R., Yoon, H.J., Ryu, H. et al. (2019). Transcutaneous ultrasound energy harvesting using capacitive triboelectric technology. *Science* 365 (6452): 491–494.

185 Lee, K.H., Zhang, Y.Z., Jiang, Q. et al. (2020). Ultrasound-driven two-dimensional $Ti_3C_2T_x$ MXene hydrogel generator. *ACS Nano* 14 (3): 3199–3207.

186 He, P., He, J., Huo, Z. et al. (2022). Microfluidics-based fabrication of flexible ionic hydrogel batteries inspired by electric eels. *Energy Storage Materials* 49: 348–359.

187 Schroeder, T.B., Guha, A., Lamoureux, A. et al. (2017). An electric-eel-inspired soft power source from stacked hydrogels. *Nature* 552 (7684): 214–218.

188 Fu, X., Zhuang, Z., Zhao, Y. et al. (2022). Stretchable and self-powered temperature–pressure dual sensing ionic skins based on thermogalvanic hydrogels. *ACS Applied Materials & Interfaces* 14 (39): 44792–44798.

189 Bai, C., Li, X., Cui, X. et al. (2022). Transparent stretchable thermogalvanic PVA/gelation hydrogel electrolyte for harnessing solar energy enabled by a binary solvent strategy. *Nano Energy* 100: 107449.

190 Liu, W., Wang, Z., Wang, G. et al. (2019). Integrated charge excitation triboelectric nanogenerator. *Nature Communications* 10 (1): 1426.

191 Wang, J., Wu, C., Dai, Y. et al. (2017). Achieving ultrahigh triboelectric charge density for efficient energy harvesting. *Nature Communications* 8 (1): 88.

192 Niu, S. and Wang, Z.L. (2015). Theoretical systems of triboelectric nanogenerators. *Nano Energy* 14: 161–192.

193 Wang, Y., Guo, T., Tian, Z. et al. (2022). MXenes for energy harvesting. *Advanced Materials* 34 (21): 2108560.

194 Yang, G., Lei, W., Chen, C. et al. (2020). Ultrathin $Ti_3C_2T_x$ (MXene) membrane for pressure-driven electrokinetic power generation. *Nano Energy* 75: 104954.

195 Cang, Y., Liu, J., Ryu, M. et al. (2022). On the origin of elasticity and heat conduction anisotropy of liquid crystal elastomers at gigahertz frequencies. *Nature Communications* 13 (1): 5248.

196 Wu, H., Yu, G., Pan, L. et al. (2013). Stable Li-ion battery anodes by in-situ polymerization of conducting hydrogel to conformally coat silicon nanoparticles. *Nature Communications* 4 (1): 1943.

197 Kim, T., Song, W., Son, D.Y. et al. (2019). Lithium-ion batteries: outlook on present, future, and hybridized technologies. *Journal of Materials Chemistry A* 7 (7): 2942–2964.

198 Wang, Z., Li, H., Tang, Z. et al. (2018). Hydrogel electrolytes for flexible aqueous energy storage devices. *Advanced Functional Materials* 28 (48): 1804560.

199 Chan, C.Y., Wang, Z., Jia, H. et al. (2021). Recent advances of hydrogel electrolytes in flexible energy storage devices. *Journal of Materials Chemistry A* 9 (4): 2043–2069.

200 Chen, Z., To, J.W.F., Wang, C. et al. (2014). A three-dimensionally interconnected carbon nanotube–conducting polymer hydrogel network for

10.1002/9783527842308.ch1, Downloaded from https://onlinelibrary.wiley.com/doi/10.1002/9783527842308.ch1 by Michigan State University, Wiley Online Library on [05/09/2024]. See the Terms and Conditions (https://onlinelibrary.wiley.com/terms-and-conditions) on Wiley Online Library for rules of use; OA articles are governed by the applicable Creative Commons License

high-performance flexible battery electrodes. *Advanced Energy Materials* 4 (12): 1400207.

201 Tian, Y. and Zhao, C.-Y. (2013). A review of solar collectors and thermal energy storage in solar thermal applications. *Applied Energy* 104: 538–553.

202 Pu, S., Liao, Y., Chen, K. et al. (2020). Thermogalvanic hydrogel for synchronous evaporative cooling and low-grade heat energy harvesting. *Nano Letters* 20 (5): 3791–3797.

203 Ding, T., Zhou, Y., Wang, X.Q. et al. (2021). All-soft and stretchable thermogalvanic gel fabric for antideformity body heat harvesting wearable. *Advanced Energy Materials* 11 (44): 2102219.

204 Lee, S.W., Yang, Y., Lee, H.W. et al. (2014). An electrochemical system for efficiently harvesting low-grade heat energy. *Nature Communications* 5 (1): 3942.

205 Han, C.-G., Qian, X., Li, Q. et al. (2020). Giant thermopower of ionic gelatin near room temperature. *Science* 368 (6495): 1091–1098.

206 Song, E., Li, J., Won, S.M. et al. (2020). Materials for flexible bioelectronic systems as chronic neural interfaces. *Nature Materials* 19 (6): 590–603.

207 Zhang, M., Tang, Z., Liu, X. et al. (2020). Electronic neural interfaces. *Nature Electronics* 3 (4): 191–200.

208 Shi, J. and Fang, Y. (2019). Flexible and implantable microelectrodes for chronically stable neural interfaces. *Advanced Materials* 31 (45): 1804895.

209 Park, Y., Franz, C.K., Ryu, H. et al. (2021). Three-dimensional, multifunctional neural interfaces for cortical spheroids and engineered assembloids. *Science Advances* 7 (12): eabf9153.

210 Son, D., Gilbert, H., and Sitti, M. (2020). Magnetically actuated soft capsule endoscope for fine-needle biopsy. *Soft Robotics* 7 (1): 10–21.

211 Erin, O., Alici, C., and Sitti, M. (2021). Design, actuation, and control of an MRI-powered untethered robot for wireless capsule endoscopy. *IEEE Robotics and Automation Letters* 6 (3): 6000–6007.

212 Mohan, S., Thirumalai, C., and Srivastava, G. (2019). Effective heart disease prediction using hybrid machine learning techniques. *IEEE Access* 7: 81542–81554.

213 Uddin, S., Khan, A., Hossain, M.E. et al. (2019). Comparing different supervised machine learning algorithms for disease prediction. *BMC Medical Informatics and Decision Making* 19 (1): 1–16.

10.1002/9783527844308.ch1, Downloaded from https://onlinelibrary.wiley.com/doi/10.1002/9783527844308.ch1 by Michigan State University, Wiley Online Library on [05/09/2024]. See the Terms and Conditions (https://onlinelibrary.wiley.com/terms-and-conditions) on Wiley Online Library for rules of use; OA articles are governed by the applicable Creative Commons License